NATIONAL AERONAUTICS AND SPACE ADMINISTRATION

Technical Memorandum 33-719

Development and Testing of the Infrared Radiometer for the Mariner Venus/Mercury 1973 Spacecraft

Theodore C. Clarke

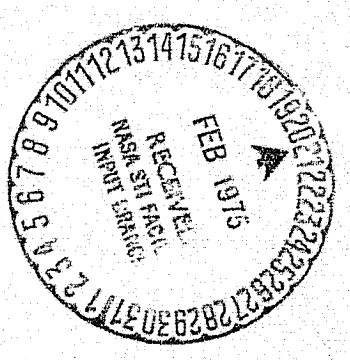

JET PROPULSION LABORATORY
CALIFORNIA INSTITUTE OF TECHNOLOGY
PASADENA, CALIFORNIA

February 1, 1975

PREFACE

The work described in this report was performed by the Santa Barbara Research Center, the Boeing Company, and the Project Engineering Division of the Jet Propulsion Laboratory under the cognizance of the Mariner Venus/ Mercury 1973 Project of the Jet Propulsion Laboratory.

ACKNOWLEDGMENTS

I gratefully acknowledge the contributions and support given me by the following people in the preparation of this report: Paul Calloway (SBRC) for contributions to the sections regarding the electronic operation of the infrared radiometer and associated bench checkout equipment; Pete Whitehead (JPL) and Al Messner (JPL) for contributions to the scan and data logic sections; Ray Becker (JPL) and Hal Nordwall (TBC) for contributions to the thermal control section; coinvestigator Ellis Miner (JPL) for contributions to and critical review of the science objectives, developmental history, and calibration sections; Clayne Yeates (JPL) for contributions to the alignment section; Mike Bender (SBRC) for contributions to the mechanical operation sections; Jack Collier (JPL) for contributions to the analog-to-pulse-width converter operation discussion; IRR Project Engineer Jack Engel (SBRC) for contributions to the subsystem test section and critical review of the whole report; Principal Investigator Stillman Chase (SBRC) for his accessibility and valuable discussions regarding key aspects of the report; the MVM '73 Nonimaging Science Payload Manager and my technical boss Dave Swenson (JPL) for his appreciation and moral support of my efforts; and finally Ray Vaughn (JPL) of Arts and Graphics for all the fine illustrations.

CONTENTS

ILLUSTRATIONS

ILLUSTRATIONS (cont)

TABLES

ABSTRACT

This report discusses the science objectives, development history, functional description, and testing of the Mariner Venus/Mercury 1973 infrared radiometer. Included in the functional description section is a thorough discussion of the IRR optical system, electronic operation, and thermal control. Signal development and its conversion to engineering units is traced, starting with the radiant space object, passing through the IRR optics and electronics, and culminating with data number development and interpretation. The test program section includes discussion of IRR calibration and alignment verification. Finally, the report reviews the problems and failures encountered by the IRR during the period of its development and testing.

1. INTRODUCTION

The Mariner Venus/Mercury 1973 infrared radiometer was designed, fabricated, and tested by the Santa Barbara Research Center under the direction of the Jet Propulsion Laboratory. The MVM IRR is similar to the type flown on the Mariner Mars '69 and '71 spacecraft, and, in addition, contains several improvements developed for the radiometers flown aboard the Pioneers 10 and 11 spacecraft.

The primary objective of the infrared radiometer experiment on board the MVM'73 spacecraft is to measure the thermal radiation from the surface of the planet Mercury between late afternoon and early morning local Mercury time (Reference 1). The secondary objective of the experiment is to perform cloud top brightness temperature measurements and limb darkening measurements at Venus. If, in addition to the latter objective, inhomogeneities in the Venusian cloud cover comparable to or larger than the instrument's resolving power at Venus (≈ 100 km) exist within the sweep of the radiometer field-of-view (FOV), it may also be possible to detect them.

There are three goals pertaining to the primary objective. They are (1) determination of the average value of the thermal inertia of the Mercurian surface material, (2) a search for anomalies or deviations from the average thermal behavior of the surface, and (3) determination of small scale inhomogeneities in the soil for different emission angles and different wavelengths.

Figure 1 illustrates the predicted diurnal equatorial surface temperatures at Mercury at a hot pole for two values of the thermal inertia , $(K\rho c)^{1/2}$, of the surface soil, where

K = thermal conductivity (J/cm-sec-°K)

ρ = density (g/cm^3)

c = heat capacity (J/g-°K)

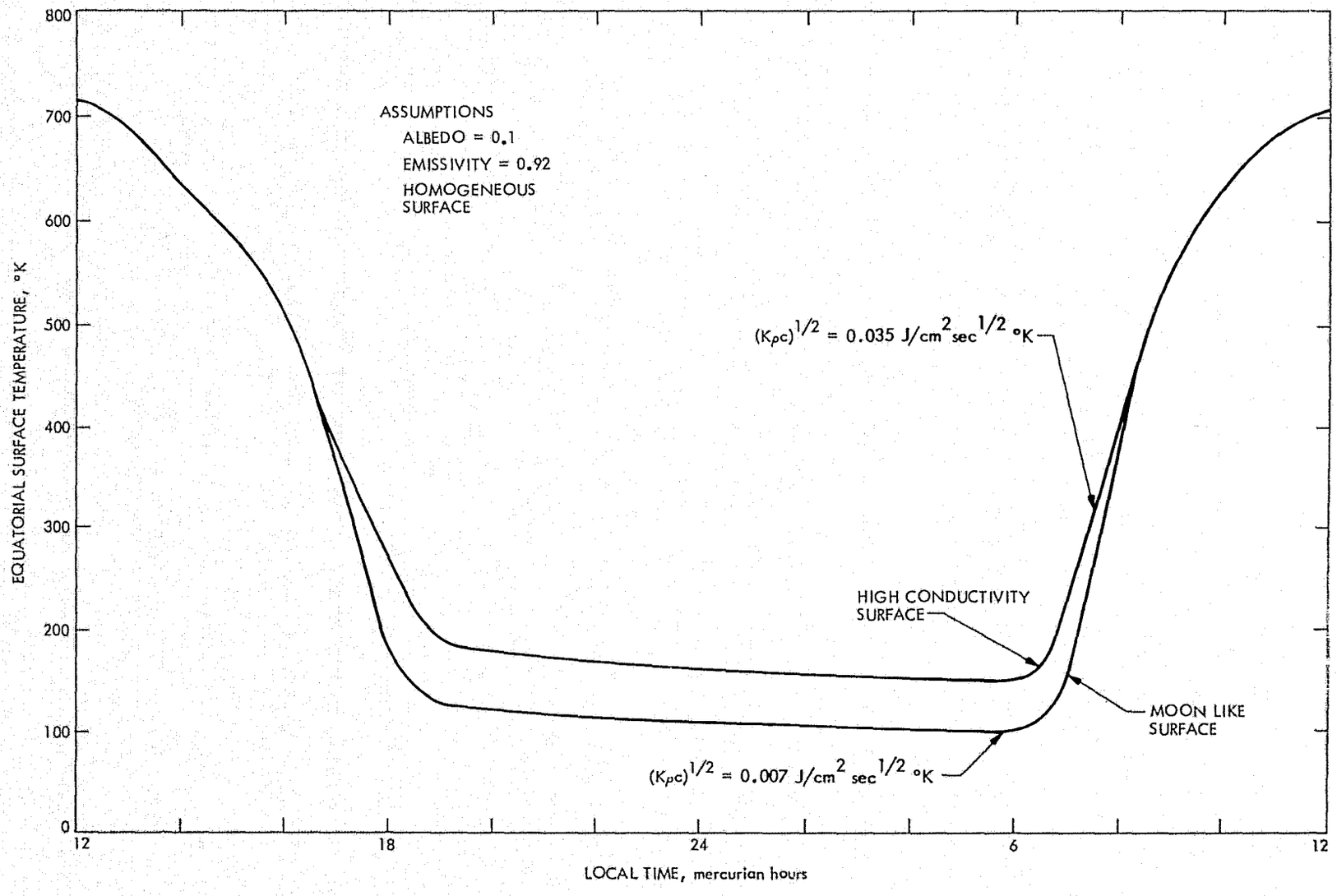

Figure 1. Model of Mercury Surface Temperature Profile

The value $(K\rho c)^{1/2} = 0.035$ J/cm^2-sec$^{1/2}$ - °K represents a relatively compact, highly conducting soil, while $(K\rho c)^{1/2} = 0.007$ is for a more nearly moon-like surface composed of a porous, highly insulating rock powder in vacuum. It should be pointed out that while Figure 1 represents the temperature profile of a single point on the planet over the period of one Mercury day (176 Earth days), the Mariner 10 IRR will make a sweep of many different points over a period of less than one hour as the spacecraft flies past Mercury. Furthermore, at the time of the Mariner 10 pass Mercury will be near aphelion when the maximum planet surface temperature is expected to be approximately 550°K.

The number and magnitude of anomalies observed on the surface of Mercury will provide a measure of the inhomogeneity of the surface. Comparison of the number of anomalies observed on Mercury and the moon will provide information on the similarities and dissimilarities of these two bodies.

Finally, variation of surface emissivity at different emission angles and different wavelengths may lead to a determination of small scale inhomogeneities in the soil. This determination will be accomplished by the IRR experiment by optically switching the FOVs of the two instrument telescopes by 120°, such that overlapping, dual wavelength band coverage of part of the planet at different emission angles will be possible.

The science team assembled to perform the MVM'73 IRR experiment is composed of experimenters who have worked together on 8 interplanetary missions and have accumulated a total of 27 man missions of flight experience in infrared radiometers, dating back to the Mariner 2 mission to Venus. Team members and their responsibilities on this experiment are given in Table 1.

Table 1. Science Team for the IRR

Team Member	Position	Responsibility
Stillman C. Chase, Jr. Project Manager/ Engineer, Santa Barbara Research Center	Principal Investigator	Team Coordination, Instrumentation
Ellis D. Miner Member Tech Staff Jet Propulsion Lab	Co-Investigator	Mission Operations, Data Reduction
David Morrison Assistant Astronomer University of Hawaii	Co-Investigator	Data Analysis and Interpretation
Guido Münch Professor of Astronomy California Institute of Technology	Associate	Team Consultant for Venus Atmosphere
Gerry Neügebauer Professor of Physics California Institute of Technology	Co-Investigator	Team Consultant for Experiment Objectives, Instrument Design, Data Reduction

2. DEVELOPMENT HISTORY

The MVM IRR combines design concepts from the Mariner Mars '69 (Mariners 6 and 7) and '71 (Mariner 9) radiometers and developments from the Pioneers 10 and 11 radiometers, with only those changes necessary to accommodate the Venus/Mercury mission added to the MVM radiometer.

The antimony-bismuth thermopile detector, used by the MVM IRR, consisting of 20 radially oriented junctions, is a simplified version of the Pioneer IRR detector design, although the Mariner '69 and '71 IRRs also used antimony-bismuth elements for their thermopiles.

Two 2.54 cm diameter aperture Cassegrainian telescopes are used in the MVM IRR, one for each spectral channel. The original Mariner '69 IRR design, used on both Mariners '69 and '71, employed telescopes with simple refracting optics. However, because of the longer wavelength and higher sensitivity requirements of the MVM IRR, reflecting optics using the reststrahlen filter concept are used.

The MVM IRR detects radiation in the two spectral bands 8.5 μm - 14 μm (channel S) and 34 μm - 55 μm (channel L), and is capable of measuring brightness temperatures in the range 80°K - 700°K. The Mariners '69 and '71 IRRs detected radiation in the spectral bands 8 μm - 12 μm and 18 μm - 25 μm and were capable of measuring brightness temperatures in the range 140°K - 325°K.

The MVM IRR uses BaF_2 reststrahlen filtration to define its channel L spectral band. The Pioneer radiometers first used the BaF_2 reststrahlen filter design.

While the Mariners '69 and '71 IRRs used square FOVs, the MVM IRR employs round FOVs, 0.5 degree round for channel S and 1.07 degree round for channel L.

The MVM IRR scan mirror stepping mechanism is similar to that used on the Mariners '69 and '71 IRRs except that 120° rather than 90° spacing between viewport detents is used in the MVM design. In addition, the MVM IRR employs a larger higher efficiency stepper motor with 60 degrees per step and

two steps between each of the view detents, reference, space, and planet. Pioneer, of course, is spin stabilized and its IRR does not use a stepper motor at all.

Except for the scan drive logic the electronic circuits in the MVM IRR have been carried over from the Pioneer IRR design.

In order to provide additional IRR status visibility and operating flexibility two innovations were incorporated in the MVM' 73 IRR. The first, a microswitch riding on the scan mirror drive shaft, has been added to provide a mirror position status bit. And lastly, the capability to reverse the roles of the planet and space ports by reversing the direction of rotation of the scan mirror thus allowing two modes of IRR operation, was added.

3. FUNCTIONAL DESCRIPTION

Portions of the descriptive material in this section are taken from the functional requirements for the IRR (Reference 2).

3.1 Optical System

The optical system of the IRR consists of the object space 45° scan mirror, two 2.54 cm diameter Cassegrainian telescopes with reflecting relay optics, and a detector assembly, including field stop and focusing lens, associated with each telescope. During normal IRR operation the 45° scan mirror is rotationally stepped in 60° step increments to 3 viewing positions, each 120° apart. The scan mirror thus views object space through the forward viewport, through the aft viewport, or towards the reference surface within the instrument itself. Figure 2, which shows the flight model IRR as it was delivered to JPL prior to system testing at Boeing, shows the scan mirror-viewport relationship. The bulge at the left end of the cylindrical optics housing in the figure is the dust cover for the stepper motor which drives the scan mirror. The two large holes in the side of the optics housing are the forward viewport. There is one hole for each of the two instrument telescopes. Symmetrically located on the opposite side of the housing and 120° from the forward viewport is the aft viewport. Through the forward viewport can be seen the backside of the scan mirror. The position of the scan mirror as seen in the figure is such that it is viewing the reference surface within the instrument. Radiation received through either of the viewports or from the reference surface is reflected off the 45° scan mirror towards the telescopes which are mounted on the opposite end of the optics housing from the stepper motor. The relationship between the scan mirror and the telescopes can be seen in Figure 3, an exploded view of the infrared radiometer.

The telescope and aft optics assembly is shown in a cut-away view in Figure 4. Each telescope has a focal length of 15.2 cm. The fields-of-view are defined by circular apertures, or field stops, placed in the focal plane of the telescope as seen in Figures 3 and 4. The secondary mirror obscures 20 percent of the incident radiation at the aperture area or entrance to the telescope. Both telescopes are aligned such that their boresights are parallel and thus their FOVs are coincident in object space.

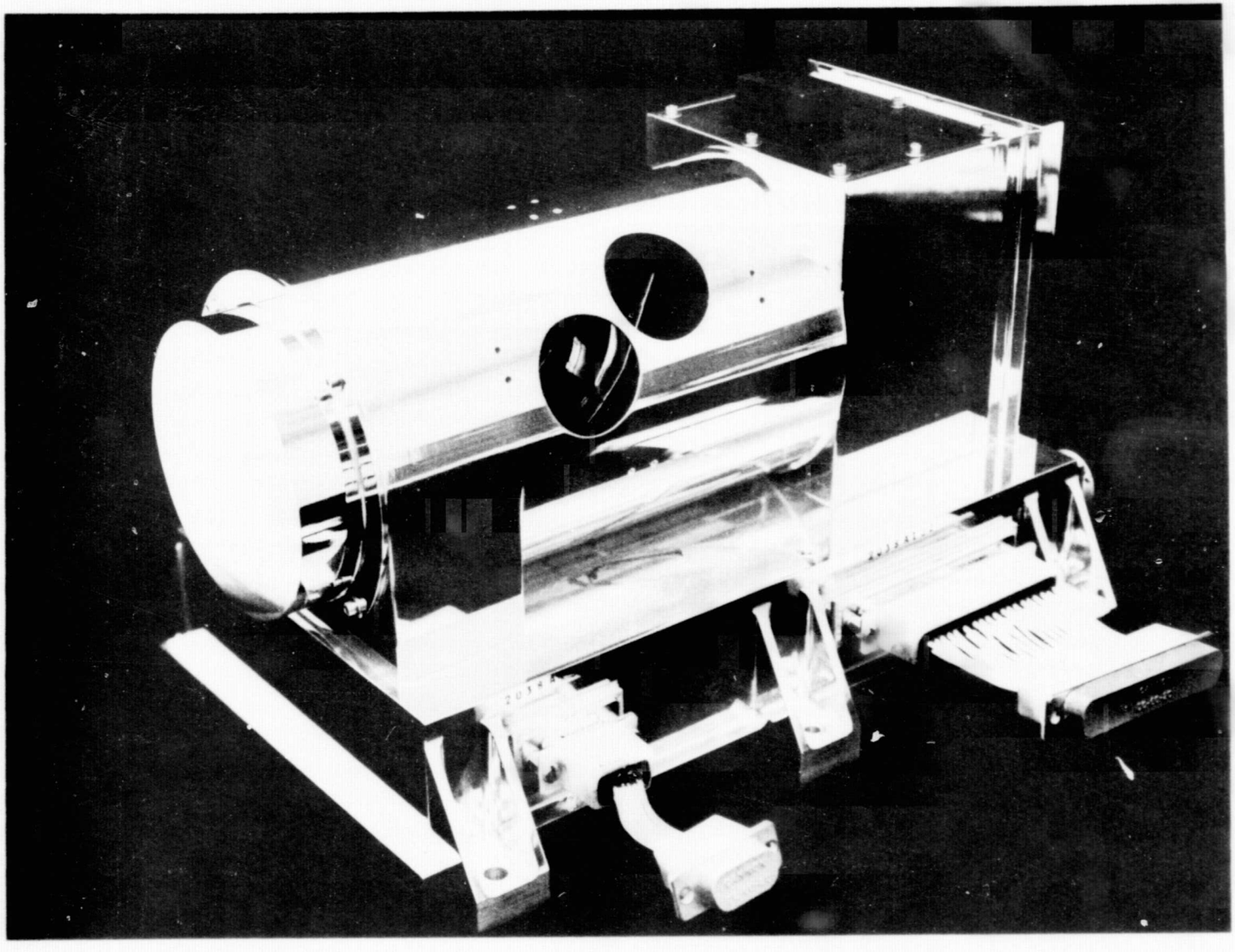

Figure 2. Infrared Radiometer Showing Scan Mirror - Viewport Relationship

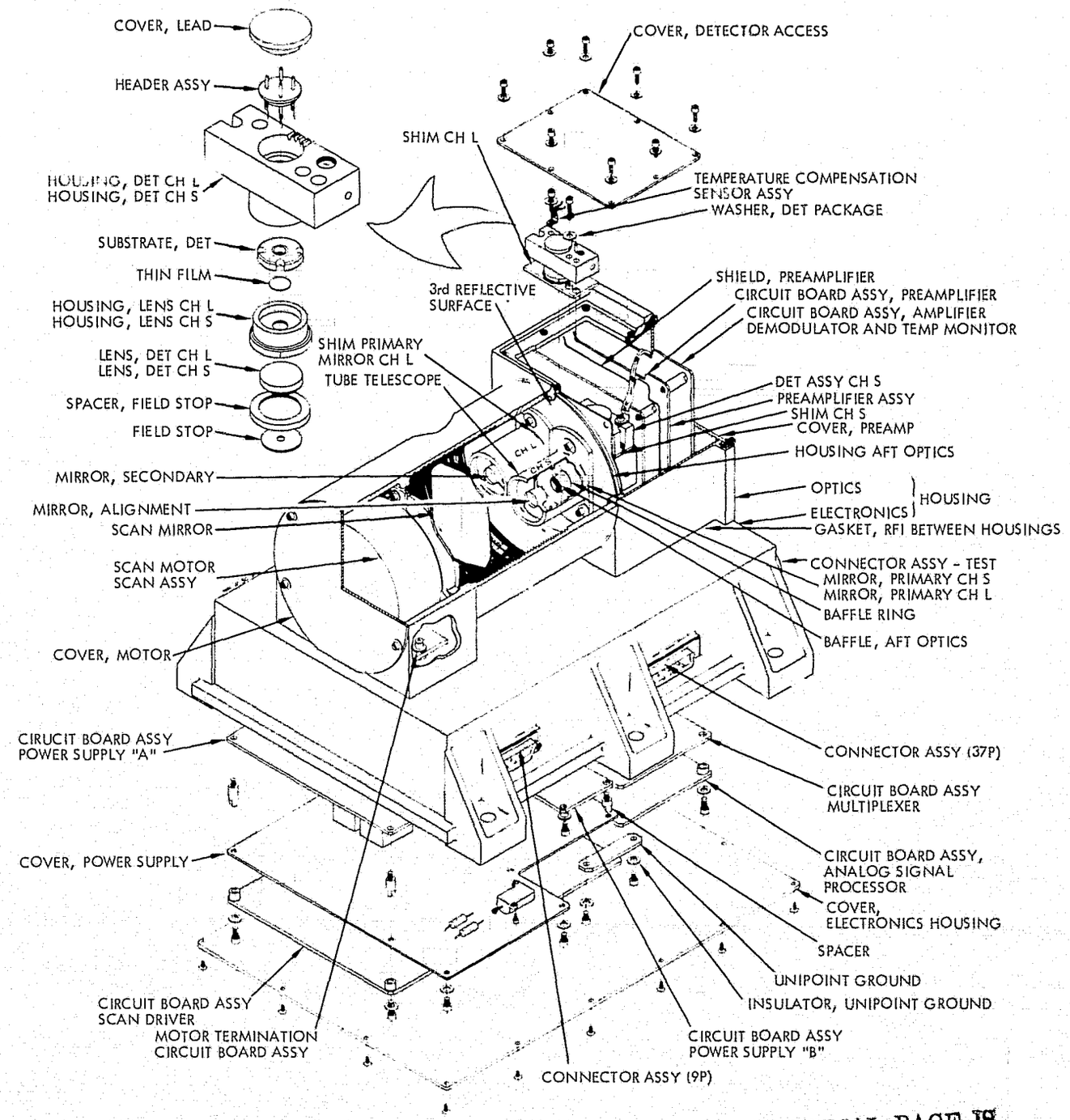

Figure 3. Exploded View of Infrared Radiometer

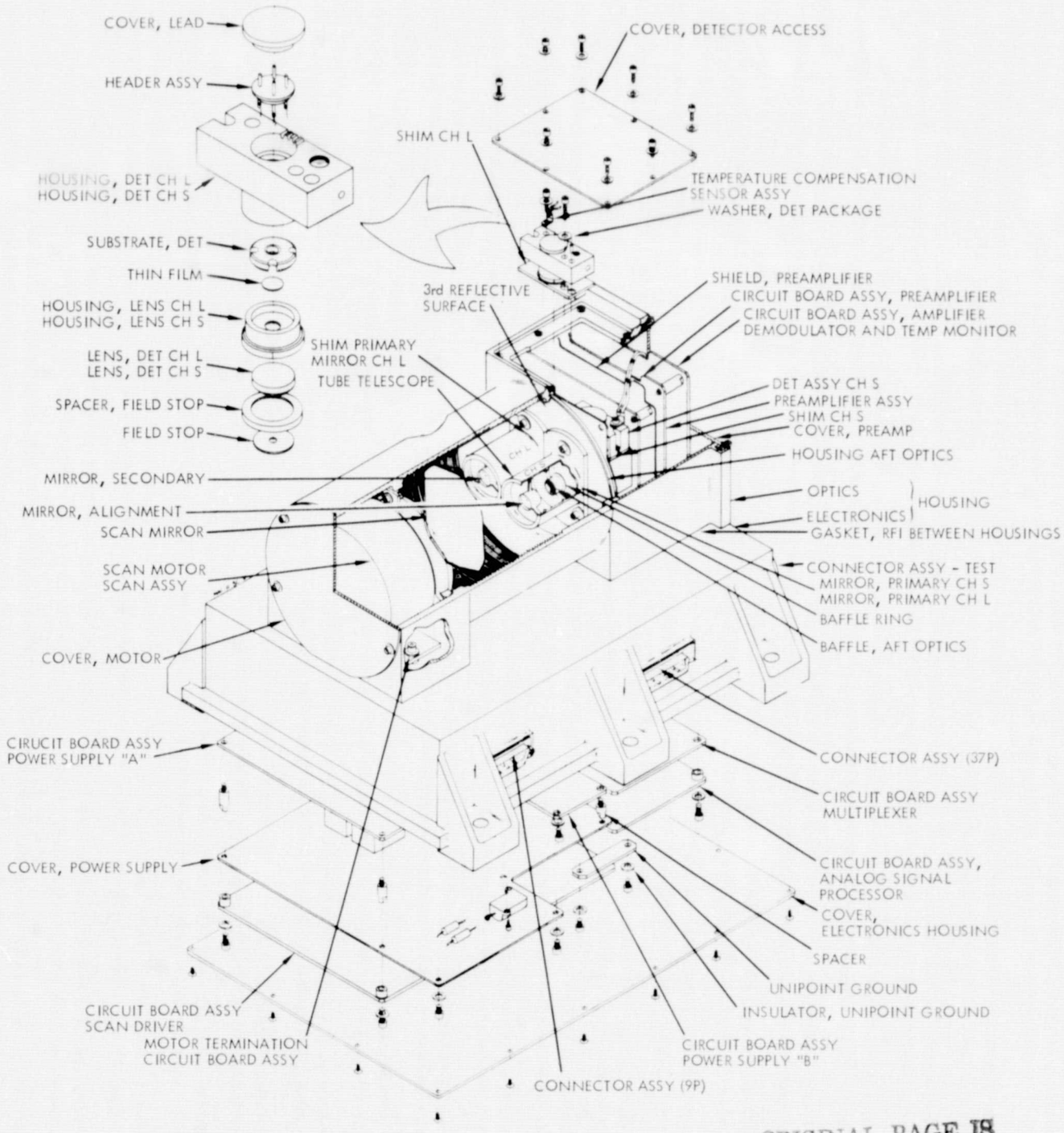

Figure 3. Exploded View of Infrared Radiometer

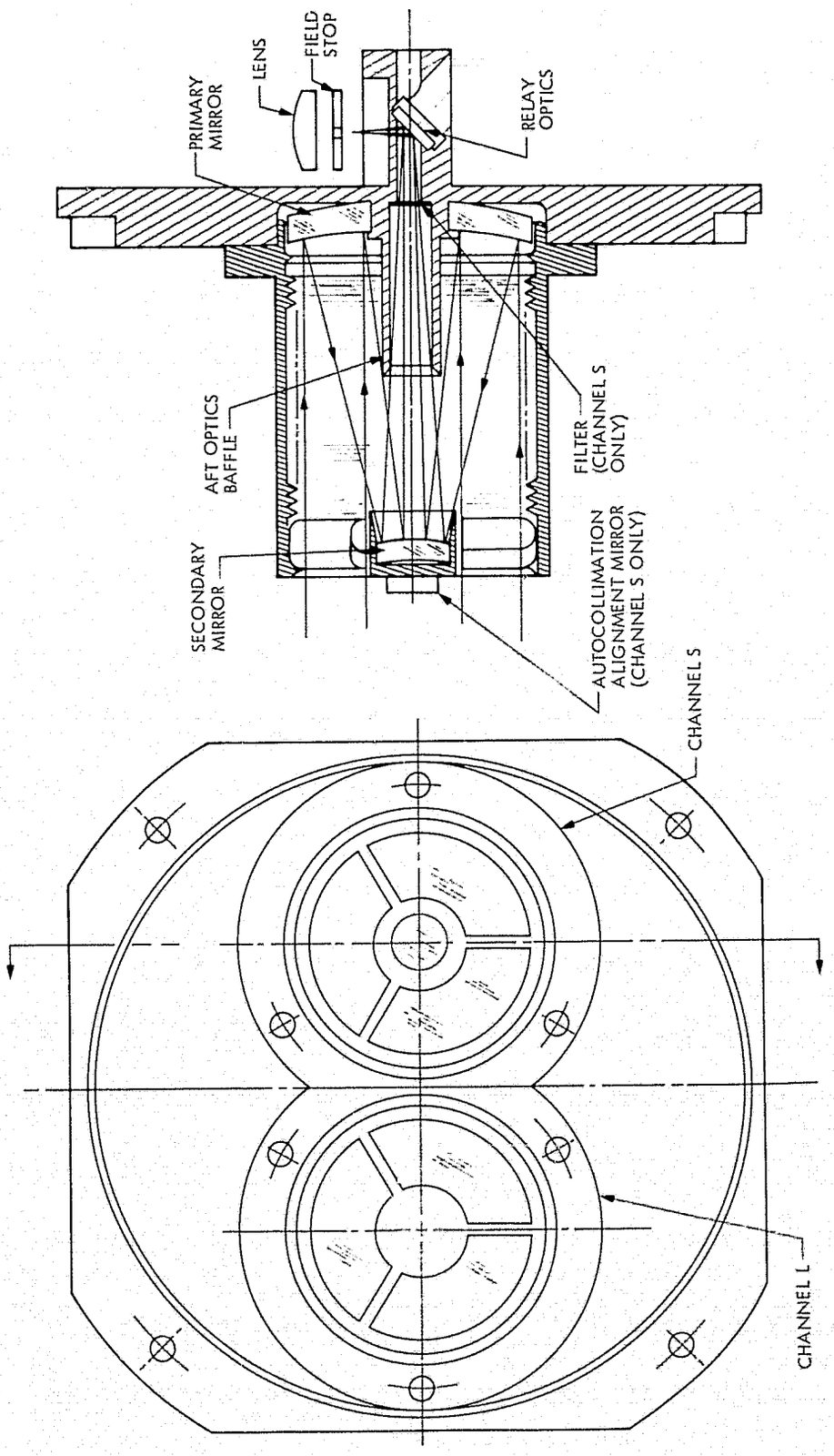

Figure 4. Telescope and Aft Optics Assembly

The channel S telescope has a 0.5 degree round FOV, defined by the field stop, while channel L has a 1.07 degree round FOV. Channel S and channel L are often referred to as channel 1 and channel 2 respectively.

The spectral bandpass of each channel is primarily defined by the telescope and aft optics associated with each channel. Channel S (S stands for "short" wavelength) employs a dielectric coated 7.6×10^{-2} cm thick Irtran 2 interference filter placed inside the aft optics baffle as shown in Figure 4. The primary and secondary mirrors and relay optics for channel S are front surface aluminized glass mirrors. After the incident beam passes through the filter it is relayed by the relay optics through the field stop and to an Irtran 4 lens which finally focuses the beam onto the channel S antimony-bismuth thermopile detector. The radiometer response curve for channel S, which takes into account not only the characteristics of the telescope optics, but also the scan mirror, lens, and blackened thermopile itself, is shown in Figure 5.

There is no transmission filter associated with channel L (L stands for "long" wavelength). Instead the bandpass for channel L is defined principally by reststrahlen reflection filtration in solid barium flouride primary and secondary mirrors and relay optics. From the relay optics the beam passes through the field stop and to a silicon lens which focuses the incident energy onto the channel L thermopile detector. The radiometer response curve for channel L, which includes the response of all optical components from the scan mirror to the channel L detector, is shown in Figure 6.

3.2 Operation

There are three operating states of the IRR. They are (1) scan mirror stepping in mode 1, (2) scan mirror stepping in mode 2, and (3) scan mirror stowed. In states (1) and (2) the flight data subsystem (FDS) sends step pulses to the IRR which cause the IRR scan mirror to step around to its three viewing positions once every 42 seconds, or once during each TV frame period. In case (3) the FDS is inhibited from sending step pulses to the IRR and the scan mirror rests stowed in the reference position.

The following discussion of the operation of the IRR includes details of the scan logic operation, data logic operation, and signal development.

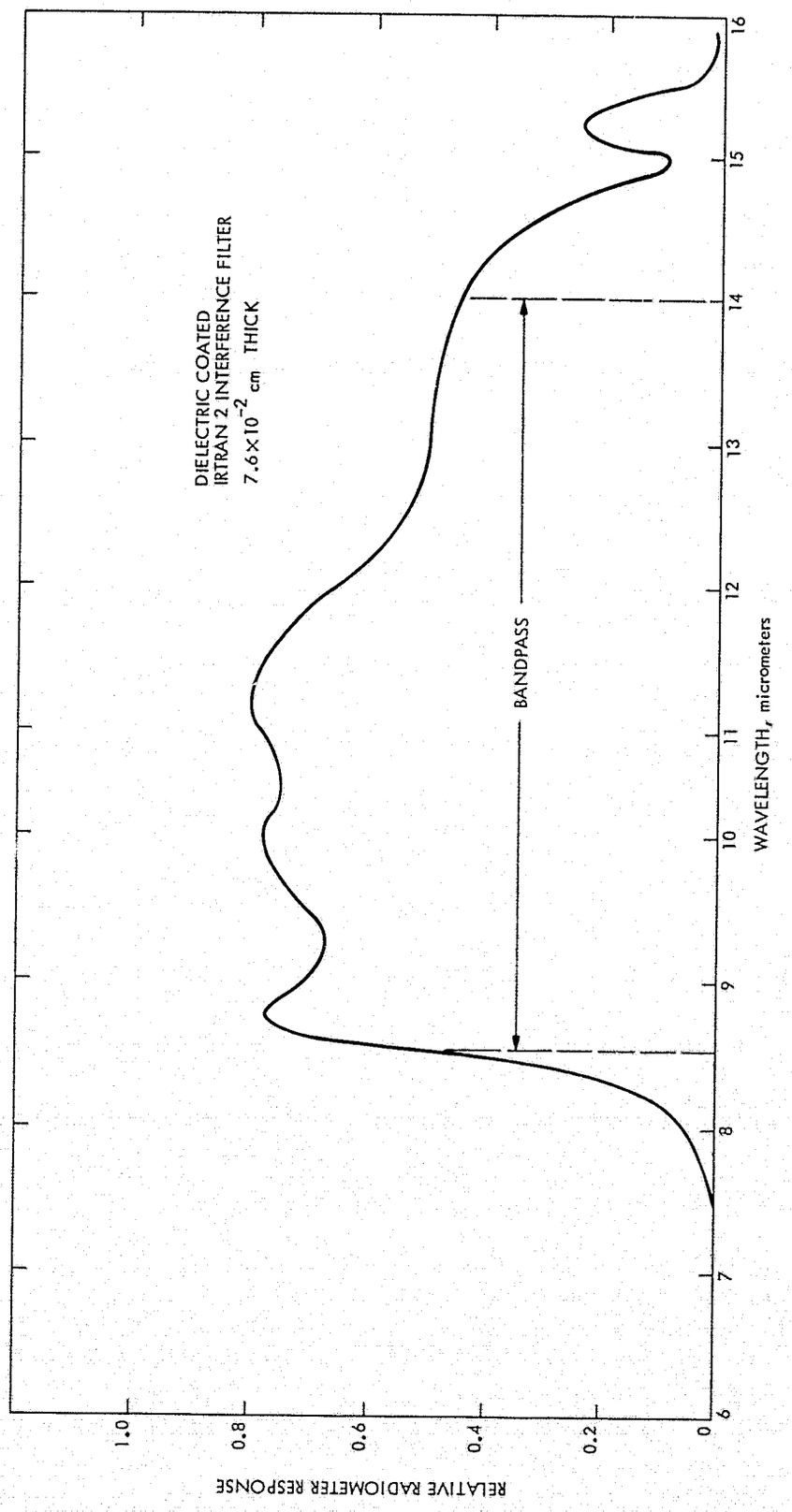

Figure 5. Radiometer Response Curve for Channel S

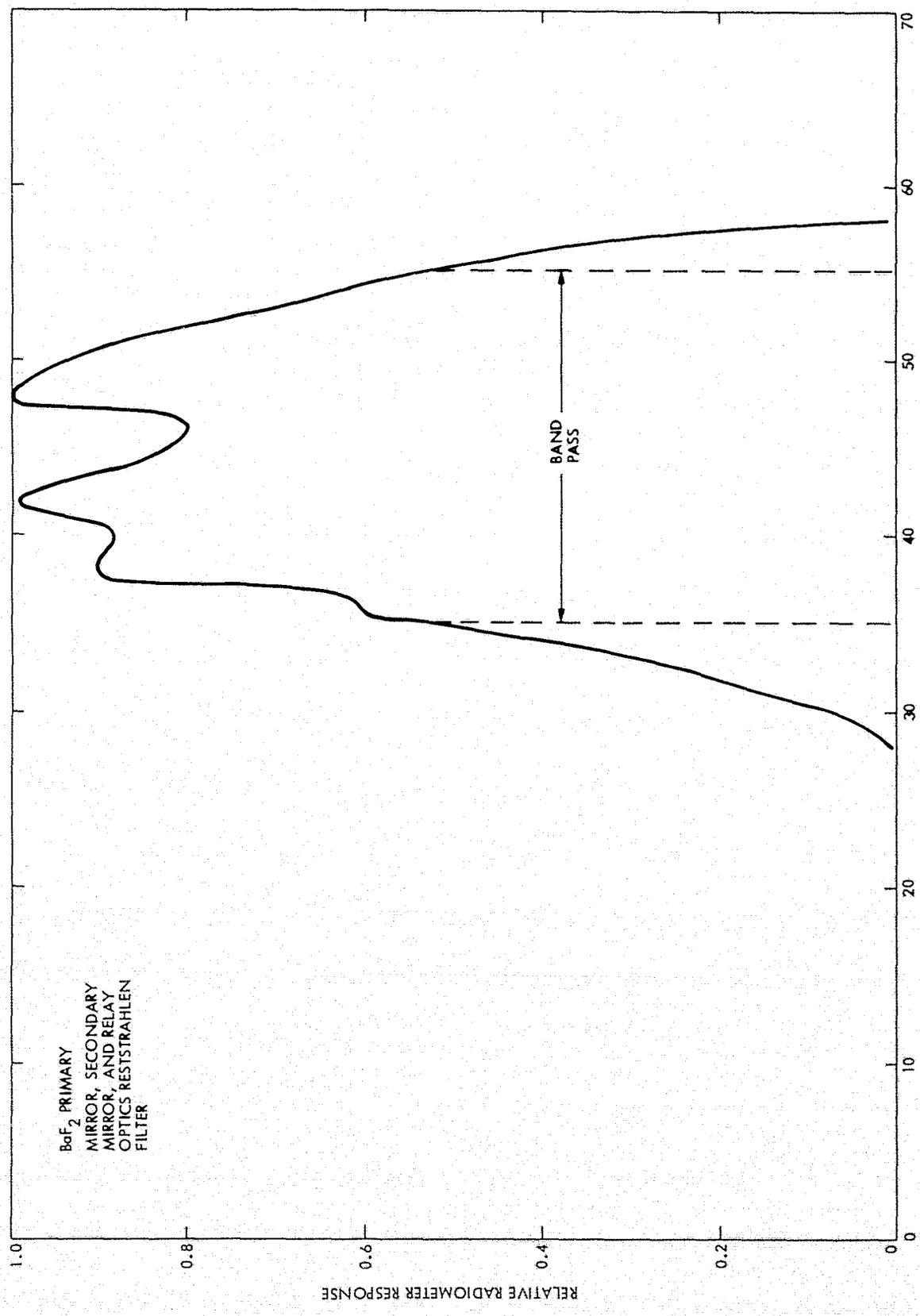

Figure 6. Radiometer Response Curve for Channel L

Frequent reference to the IRR circuit block diagram, shown in Figure 7, is made.

3.2.1 Scan Logic. When the IRR is in a stepping mode step pulses are sent from the FDS to the IRR which control the position of the IRR scan mirror. The scan mirror occupies three positions, 120° apart, during its normal 42 second cycle of operation (Reference 3). The timing of this scan cycle is illustrated in Figure 8. All time intervals specified between pulses sent by the FDS are referenced from trailing edge to trailing edge.

Each step scan pulse sent to the IRR will cause the IRR stepping motor to move the scan mirror 60°. Thus, a pair of pulses are required to advance the scan mirror one full position. There are 180 msec between pulses in each pair of step scan pulses. These pulses will not be sent by the FDS when the scan mirror is in the reference position and the FDS is commanded to stow the mirror.

The scan drive logic circuit within the IRR (Figure 7) accepts the step scan pulses from the FDS. A six state shift counter is shifted by the scan pulses to sequentially pulse the scan motor windings. The scan motor itself is a six coil stepper motor which moves in 60° increments as the coils are pulsed. The motor driver circuit rectifies the input 2400 Hz power from the spacecraft 2400 Hz inverter and stores the energy for the pulsed motor load on capacitors. These capacitors reduce the input peak power demand on the spacecraft inverter. The coil pulse duration is set by a counter within the scan drive logic circuit. This counter, keyed to the 2400 Hz inverter (one period 0.416 msec), is activated by the scan step pulse from the FDS and counts for 128 clock periods before terminating the step pulse. Thus, the step pulse from the FDS, which is 10 msec in duration, is stretched by the IRR to 53.4 msec duration. The stepper motor coils are logically numbered from 0 to 5 and are activated in ascending order. The number scheme shown in Figure 8 as being associated with mode 1 is translated to the order shown for mode 2 upon receipt of a mode 2 command. Because of logic within the FDS, the mode change takes effect at the first mode command pulse after the TV frame start, or 0.960 seconds after the second pulse in the pair of step scan

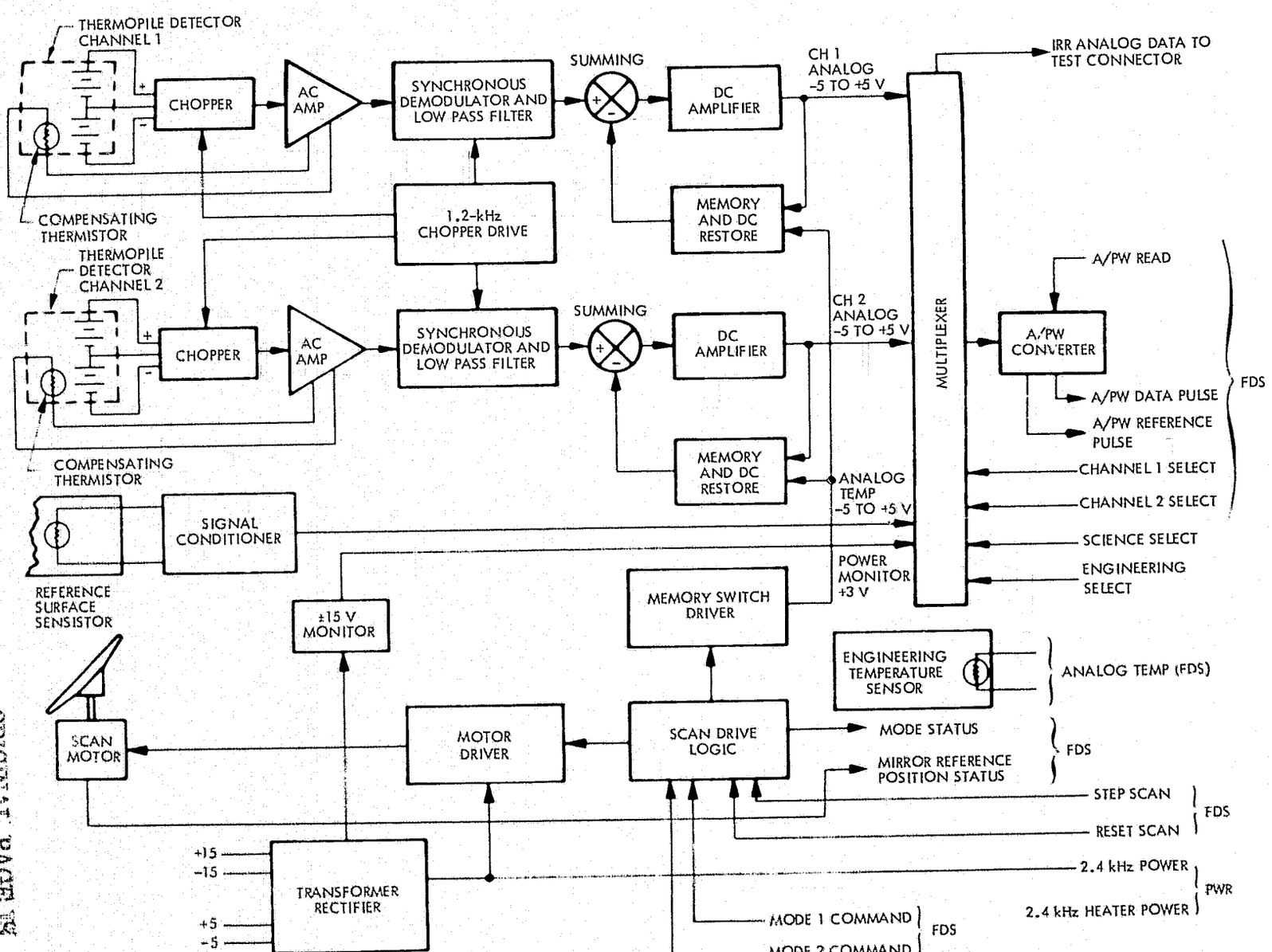

Figure 7. Circuit Block Diagram of the Infrared Radiometer, MVM73

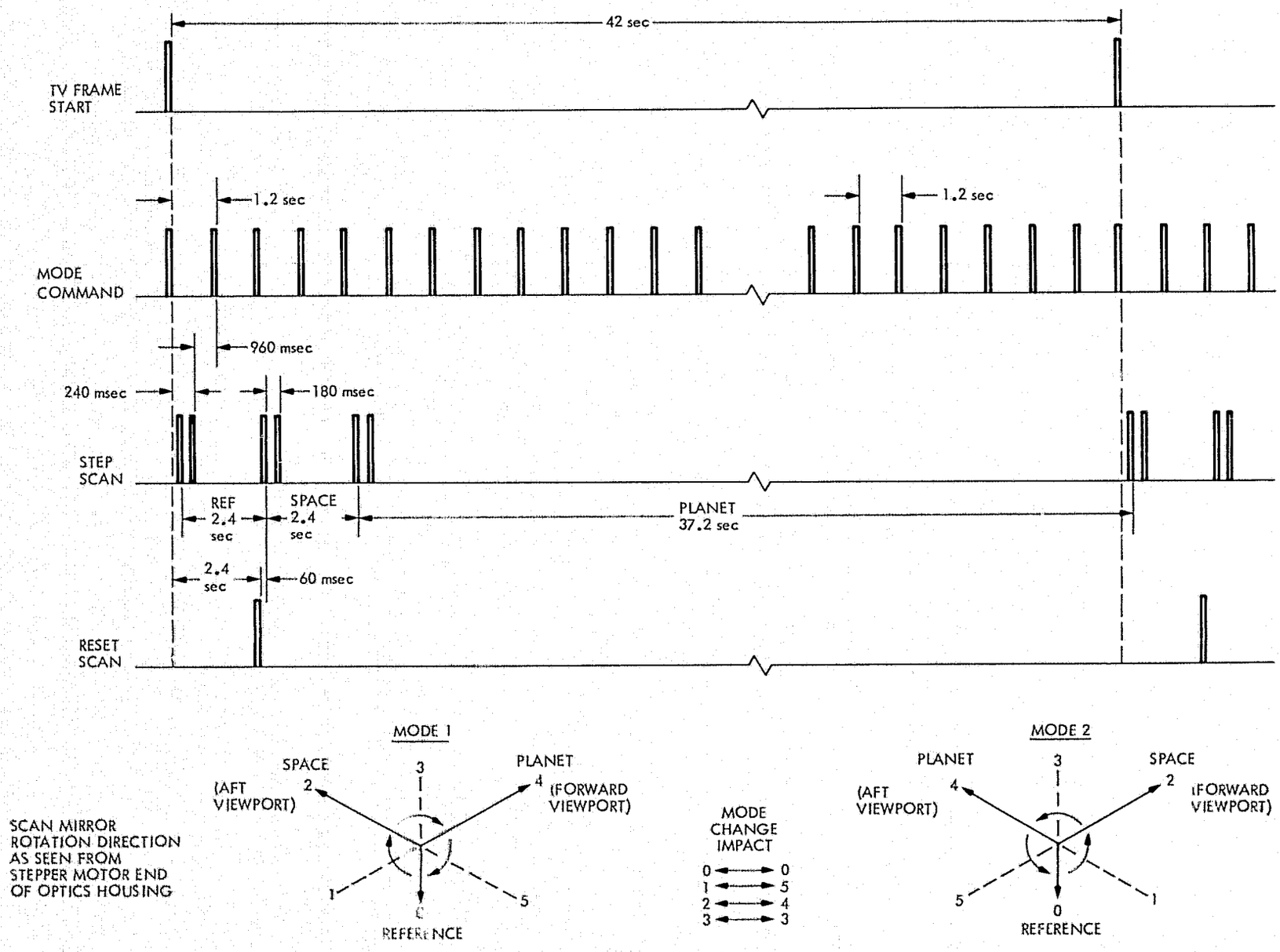

Figure 8. IRR Scan Mirror Logic Timing Diagram

pulses which move the scan mirror to the reference position. The coil number identifier for the reference position for both mode 1 and mode 2 is "0." Looking into the IRR from the motor end of the optics housing the mirror steps in a clockwise direction in mode 1 and counterclockwise direction in mode 2.

A scan reset signal to the IRR from the FDS resets the shift counter once every 42 seconds so that the scan sequence will be properly resumed even if a scan pulse is lost. The reset scan pulse occurs 60 msec before the first pulse in the pair of step scan pulses which move the scan mirror to the space position. These reset pulses will always be sent by the FDS to the IRR even if the scan mirror is stowed. The second state of the shift counter normally corresponds to the scan mirror being in the space look position regardless of the direction of scan mirror rotation. A set of gates within the scan drive logic circuit activates the dc restore circuits for both spectral channels when the shift counter is in its second state, defined as the space position. The dc restore function will be discussed in Section 3.2.3, Signal Development.

3.2.2 Data Logic. In any full 42 second TV frame period the IRR provides 34 science data samples and one engineering data sample from each of its two spectral channels to the FDS for eventual downlink transmission. The IRR logic circuit that selects which data signal to process in the analog-to-pulse-width (A/PW) converter, and send to the FDS, is the multiplexer, as seen in Figure 7. The multiplexer itself is controlled by data select signals from the FDS. The timing of these data select signals is illustrated in Figure 9.

The data select signals from the FDS are routed to two latch circuits within the multiplexer, one for engineering data and one for science data. Each of these latch circuits in turn provides two logic level signals, one for channel 1 data and one for channel 2 data. These four logic levels provide gate signals to four J-FET switches. Only one of these switches can be on at a time, switching the analog signals, developed by the radiometer, to the A/PW converter, all in accordance with the FDS data select signals.

Each science select signal from the FDS to the IRR selects a pair of IRR science data samples, one sample from each IRR channel, for conversion by the A/PW converter. There are 34 of these signals to the IRR every

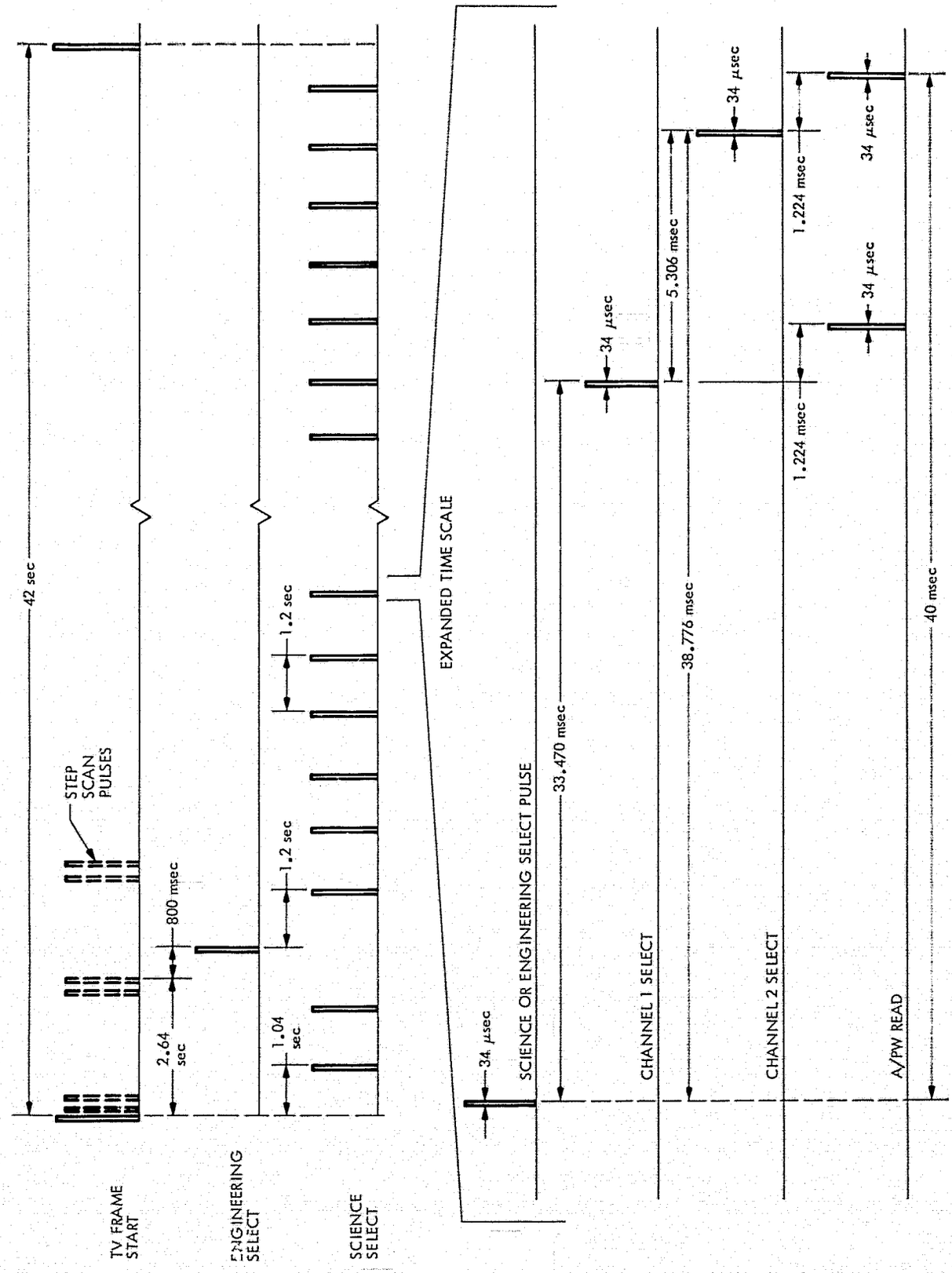

Figure 9. IRR Data Logic Timing Diagram

42 seconds. They occur 1.2 seconds apart except where they are interrupted by the engineering select signal, in which case the flanking science select signals are 2.4 seconds apart.

Each engineering select signal selects a pair of IRR engineering data samples, one per channel, for A/PW conversion. The channel 1 sample is a thermistor measurement of the IRR thermal reference surface. The channel 2 sample is a measurement of the IRR power supply voltage. There is one engineering select signal from the FDS to the IRR every 42 seconds. This signal occurs 800 milliseconds after the second pulse in the pair of step scan pulses which step the IRR scan mirror to the space position. It can be seen that of the two pairs of data samples selected for A/PW conversion when the IRR scan mirror is in the space position the first pair are engineering measurements, while the second pair are space measurements. The science select signal which occurs when the IRR mirror is in the space position does so 220 milliseconds before the first pulse in the pair of step scan pulses which step the IRR scan mirror to the planet position.

The timing of the channel select signals and A/PW read signals from the FDS to the IRR multiplexer and A/PW converter, respectively, relative to the science or engineering select signals, is shown in Figure 9. The channel select signals open the gate between the IRR signal development electronics and the A/PW converter thus enabling the A/PW converter to look at the selected channel, while the A/PW read signal, which occurs 1.224 milliseconds after the channel select signals, actually initiates an A/PW conversion. Signal development and A/PW conversion is the topic of the next section in this report.

3.2.3 Signal Development. Energy from object space is relayed by the IRR optical system to two identical thermopile detectors, one for each channel. Each detector is a 20 junction center-tapped antimony-bismuth thermopile, 0.05 cm in diameter, with the junctions arranged radially. The detectors are connected to the preamplifier inputs (see Figure 7) through switching FETs which alternately reverse the polarity of the detector signals applied to the differential preamplifier inputs. The switching FETs provide a 1200 Hz chopped squarewave input to the preamplifiers. The 1200 Hz chopper

drive signal is itself provided by the IRR power supply which electronically divides down the input 2400 Hz squarewave spacecraft power.

After amplification in the preamplifier, the chopped detector signal is further amplified in the ac amplifier circuit. The demodulator circuit then shifts the ac signal to a ground referenced pulsating dc signal, which is then operated on by the low pass filter amplifier. The output of the low pass filter amplifier is dc with little residual ripple.

The dc signals from the filter amplifier circuits of both channels are further amplified in the dc amplifier circuits. During the space viewing interval, determined by the scan logic as discussed in Section 3.2.1, the signal value at the dc amplifier output is stored on a memory capacitor in the dc restore circuit feedback loop. Since the temperature of space is near absolute zero the signal stored on the memory capacitor is equivalent to the thermal and electrical offsets in the system. Furthermore, a -5 volt reference at the input to the feedback amplifier causes the loop to dc restore to -5 volts during the dc restore period, which only occurs during the space viewing interval. This -5 volts sets the minimum pulse period for the A/PW converter. At the end of the dc restore period the scan mirror steps around to view the planet and reference surface. The thermal and electrical offset signal stored on the memory capacitor is subtracted from the signal generated while viewing either the planet from the opposite port or the reference surface, since the offsets would appear on the latter signals also. Thus, the resulting analog signal input to the A/PW converter is due primarily to radiation falling on the detector from object space only. If the thermal offset caused by one port is different from that caused by the opposite port then the difference can be determined simply by comparing the planet data obtained in mode 1 with that obtained in mode 2 when both ports see only space, such as during a nonencounter inflight functional check. If the offsets are the same then the analog signal will vary from -5 volts for a signal equal to that received while viewing space to +5 volts for the signal received while viewing the highest temperature within the dynamic range.

The amplified dc analog signals are input to the multiplexer for sampling, determined by the FDS as discussed in Section 3.2.2, and then conversion by the A/PW converter. The output of the A/PW converter is

two pulses. The time between the two pulses is proportional to the value of the input analog dc signal. The A/PW converter input voltage is limited to ±5.6 volts dc, although the dynamic range of the IRR effectively limits signals to the ±5 volt range. The functional operation of the A/PW converter can be understood from Figure 10 and is described below (Reference 4).

An A/PW "read" command signal is generated by and sent from the FDS to the IRR 1.224 milliseconds after every channel select signal, as shown in Figure 9. This negative command signal triggers a negative going voltage ramp internal to the A/PW converter. The ramp starts at approximately +7.5 volts and decreases linearly to approximately -6.5 volts at which point the A/PW converter resets itself and is then ready to perform another conversion. This ramp is compared internally to both the analog voltage signal, which was switched by the multiplexer from the output of the channel being sampled to the input of the A/PW converter, and to the ground reference. If it is assumed, for example, that the analog input signal is positive, as shown in Figure 10, then, as the ramp passes through that voltage which is equal to the analog input signal a positive "data" pulse is generated by the A/PW converter and is coupled out of the converter to the FDS. This "data" pulse starts a 9-bit accumulator (binary counter) in the FDS which counts at a rate of 470.4 kHz. The ramp voltage continues to fall towards its reset value of -6.5 volts. As the ramp passes through that voltage which is equal to ground reference (zero volts) a positive "reference" pulse is generated by the A/PW converter and is coupled out of the converter to the FDS. This "reference" pulse stops the accumulator. The resultant count in the accumulator represents the time between the "data" pulse and "reference" pulse and is directly proportional to the analog dc voltage signal input. The count in the accumulator also becomes the nine least significant bits of each 10-bit IRR data word in the non-imaging science 1 (NIS-1) format. The most significant bit of each of these words is the sign bit. Data is positive in sign when the A/PW "data" pulse is received by the FDS before the A/PW "reference" pulse. This corresponds, as in the example just discussed, to a positive analog input signal. In the case of a negative analog input signal, the "reference" pulse will be coupled out of the A/PW converter first, and it will start the 9-bit accumulator. The "data" pulse, which would be generated by the A/PW converter and coupled

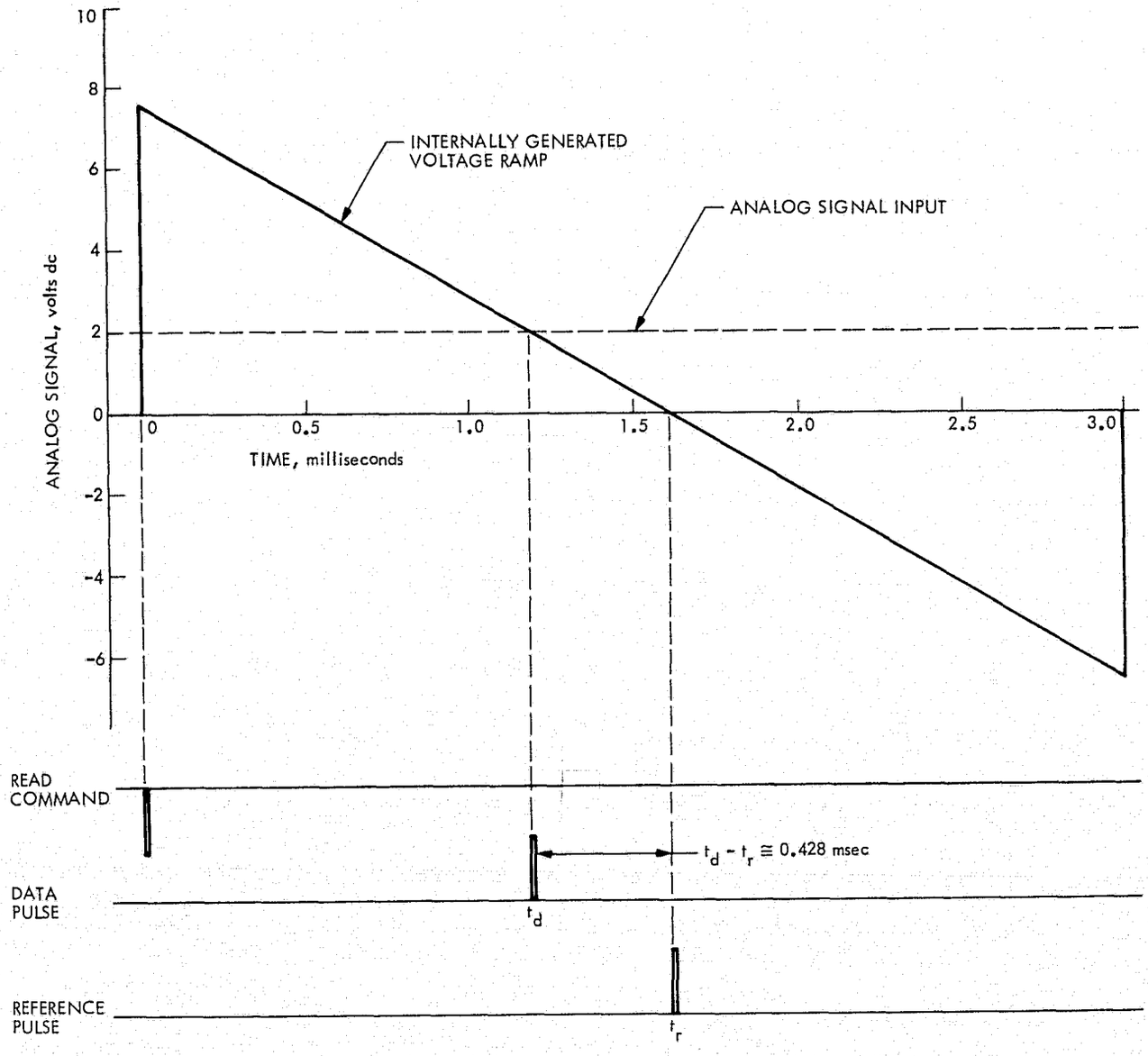

Figure 10. IRR A/PW Converter Operation for Positive Analog Signal Input

out to the FDS after the "reference" pulse would stop the accumulator in this case.

The maximum count in an IRR word is ±511 data numbers (DN), although the absolute zero reference for the space sample is set at -498 DN to allow for possible thermal and electrical offsets. 2.14 microseconds between the A/PW "data" and "reference" pulses corresponds to a 10 millivolt analog signal and also to a one DN count on the 9-bit accumulator. As an example, for a +2.0 volt analog signal, as shown in Figure 10, the time between A/PW pulses would be approximately 428 microseconds, and the IRR data word on the FDS accumulator would be approximately +200 DN. What this means in terms of object temperature will be discussed briefly in Section 4.1, Subsystem Tests and Calibration.

The circuits which provide the engineering measurement signals to the multiplexer for input to the A/PW converter are shown in Figure 7 as the reference surface sensistor for the temperature measurement, and the ±15 volt monitor for the power supply voltage measurement. The temperature monitoring circuit uses a positive temperature coefficient silicon sensistor bonded into a hole in the reference surface for the temperature measurement. The signal conditioner is set so that the minimum measurable temperature of about -40° C provides an analog signal input to the A/PW converter of -5 volts. The amplifier gain in the signal conditioner is also set so that the high end of the temperature range of interest (~+65° C) provides a +5 volt analog signal. Finally, the ±15 volt outputs are applied to a resistor divider network for monitoring as the engineering data measurement in channel 2.

3.3 Thermal Control

In order to maintain the temperature of the IRR within the limits established during the program, shown in Table 2, throughout the duration of the mission, extensive thermal control measures were put into effect. Figure 11 shows the principal heat paths to and from the IRR expected during the mission.

The main source of heat into the IRR is the spacecraft power supply. Depending on what state it is in the IRR dissipates between 2.21 and 2.7 watts

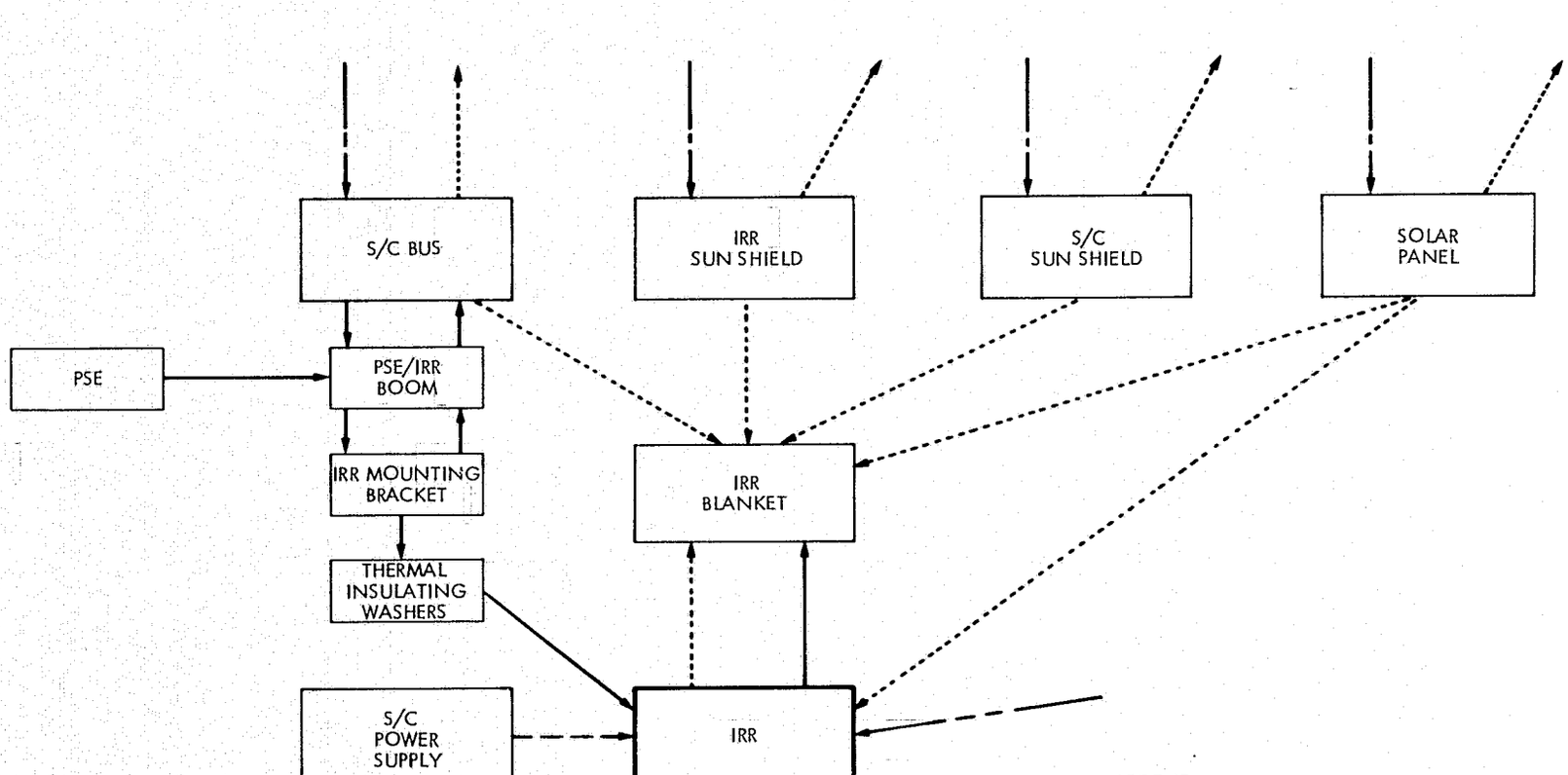

Figure 11. IRR Temperature Control Functional Diagram

Table 2. IRR Instrument Temperature Ranges

Description	Temperature Limits
1. Desired Encounter Range	-10°C (+14°F) to +30°C (+86°F) (Reference 2)
2. Nominal Operating Range	-15.5°C (+4°F) to +35.5°C (+96°F) (Reference 2)
3. Calibrated Operating Range	-20°C (-4°F) to +40°C (+104°F) (Reference 5)
4. Flight Acceptance (FA) Operating Range	-20°C (-4°F) to +40°C (+104°F) (Reference 6)
5. Type Approval (TA) Operating Range	-20°C (-4°F) to +40°C (+104°F) (Reference 6)
6. Nominal Storage Range	-30°C (-22°F) to +50°C (+122°F) (Reference 2)
7. FA Storage Range	-1°C (-34°F) to +50°C (+122°F) (Reference 6)
8. TA Storage Range	-45°C (-49°F) to +60°C (+140°F) (Reference 6)

of electrical power furnished by the spacecraft power supply (Reference 7). When IRR power is on, the IRR electronics dissipates 2.21 watts when operating in mode 1 or mode 2 stepping, and 2.7 watts when stowed. When IRR power is off the IRR replacement heater dissipates 2.5 watts.

There is a strong thermal interaction between the PSE and IRR (Reference 8) since both are mounted on the PSE/IRR boom, as shown in Figure 12. When the PSE supplemental heater (9.2 watts) is turned off the solar thermal vacuum tests showed (Figure 13) that the IRR would drop 25°F in temperature even though the IRR was thermally isolated as much as possible from the PSE by mounting both instruments on insulating washers.

Another important thermal input to the IRR is thermal radiation from the -X solar panel. This input becomes particularly important as the spacecraft moves closer to the sun and the solar panels are tilted so that the -X panel surface is more nearly normal to the IRR. The major thermal contribution from this source is the radiation entering the IRR aft viewport.

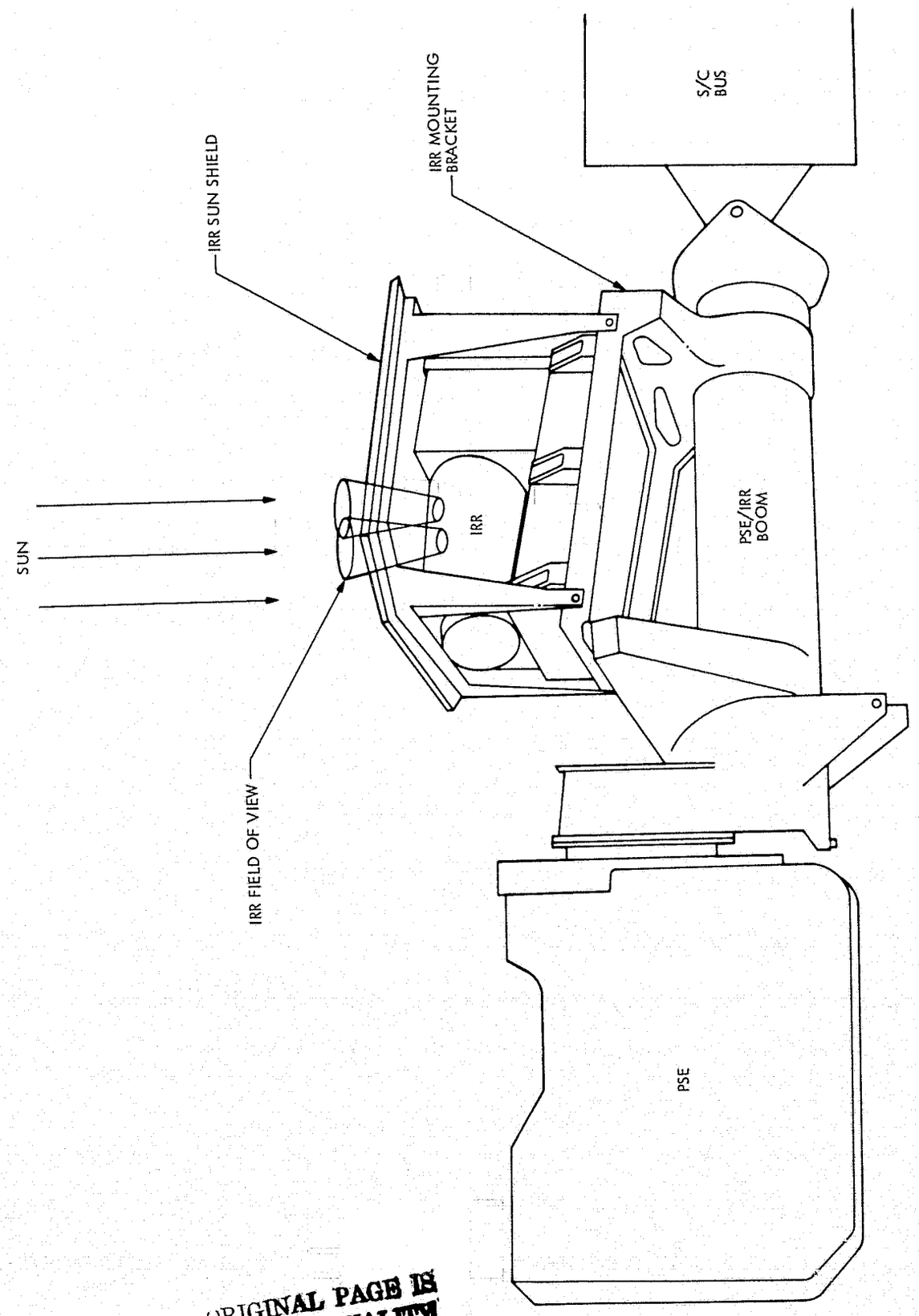

Figure 12. IRR Mounting Configuration

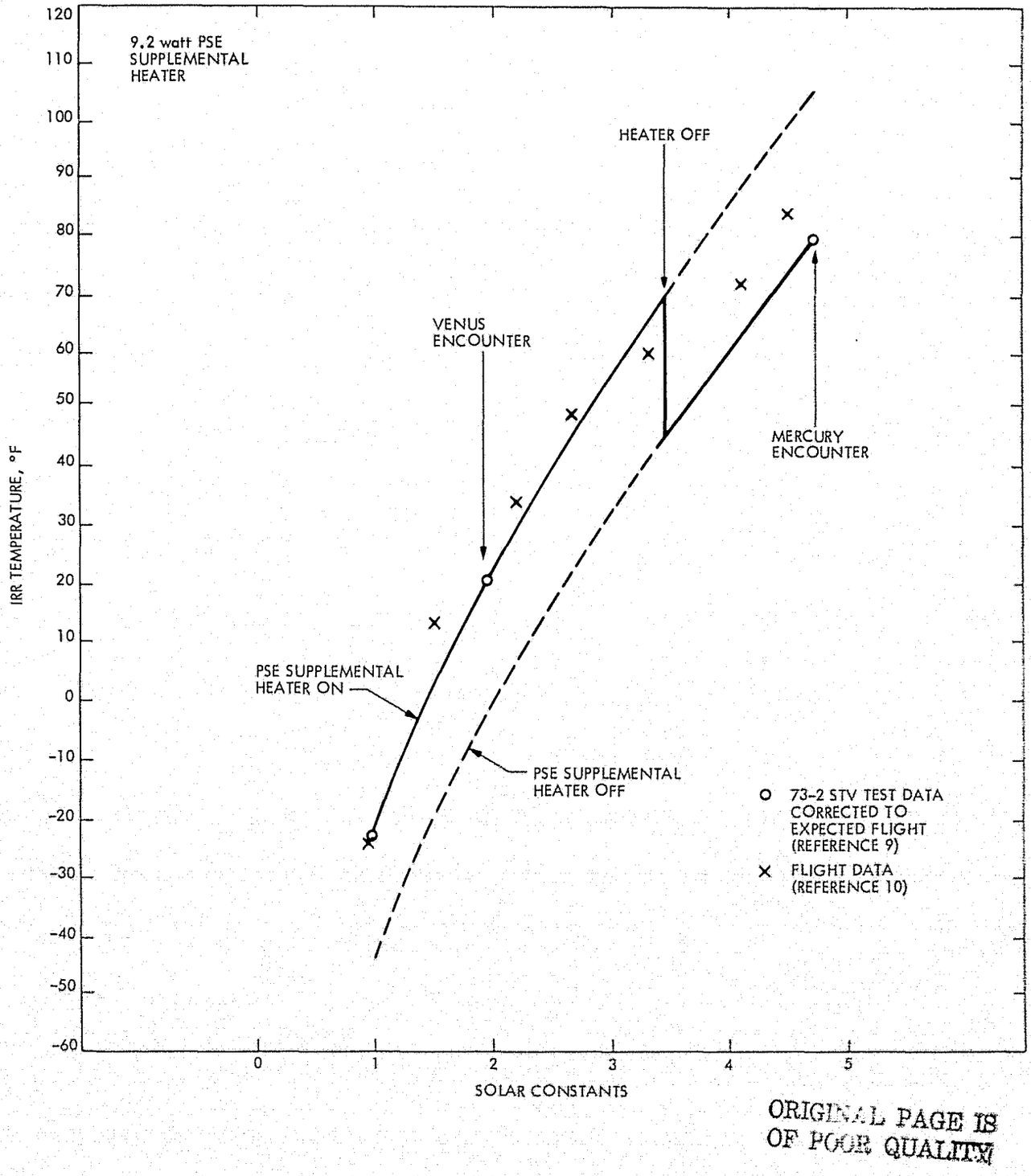

Figure 13. Predicted IRR Flight Temperatures

The IRR uses four methods to control and regulate its temperature. First, the instrument itself is constructed of aluminum with its outer surface highly polished, as seen in Figure 14. This surface has a reflectivity over the solar spectrum of near unity. However, because in its flight configuration the IRR is covered by a thermal blanket and shaded by its own sunshield, as shown in Figure 15, the highly reflective instrument surface provides backup protection only, in case, for example, of a blanket tear during the mission.

The IRR thermal blanket is the second method of thermal control. From the outer surface in, it consists of 1 layer of 2.54×10^{-3} cm thick aluminized teflon, teflon side out, 3 layers of 1.27×10^{-3}cm thick crinkled goldized kapton, kapton side out, 10 layers of 0.32×10^{-3} cm thick double aluminized mylar alternated with 9 layers of 22.8×10^{-3} cm thick nylon scrim, 1 layer of dacron filter cloth, and finally, 1 layer of 2.54×10^{-3} cm thick aluminized teflon, with the teflon side against the instrument to prevent electrical shorting. The blanket seams are made of fibreglass and sewn together with dacron thread. The blanket is fitted and tied down about the viewports using dacron thread passed through the blanket tie down holes, which can be seen in Figure 14.

The third thermal control method is the IRR sunshield. It is used to prevent long term solar exposure of the IRR thermal blanket, and also to keep direct solar radiation out of the IRR viewports. The outer layer of the sunshield is beta cloth, which is a teflon impregnated glass cloth, and it is followed by multiple layers of aluminized teflon, aluminized mylar, and nylon scrim. The bottom 2 layers are dacron filter cloth and goldized kapton, with the kapton facing the instrument.

The fourth and most active thermal control technique used on the IRR is radiative cooling. The IRR mounting bracket is a car battery holder type bracket, which allows the IRR base plate to view space. This base plate is painted with a 3.8×10^{-3} to 7.6×10^{-3} cm thick coating of Dow Corning 92-007 white silicone paint to permit T^4 radiative cooling of the IRR. The paint has a high emissivity over the black body spectrum centered around 300° K, which is the nominal IRR temperature for the latter part of the mission. The entire bottom surface of the plate is painted except for a 1.9 cm wide strip around the plate rim. The 21.3 cm by 12.2 cm painted area is masked off to a total

Figure 14. IRF Mounted, Before Thermal Blanket and Sunshield Installation

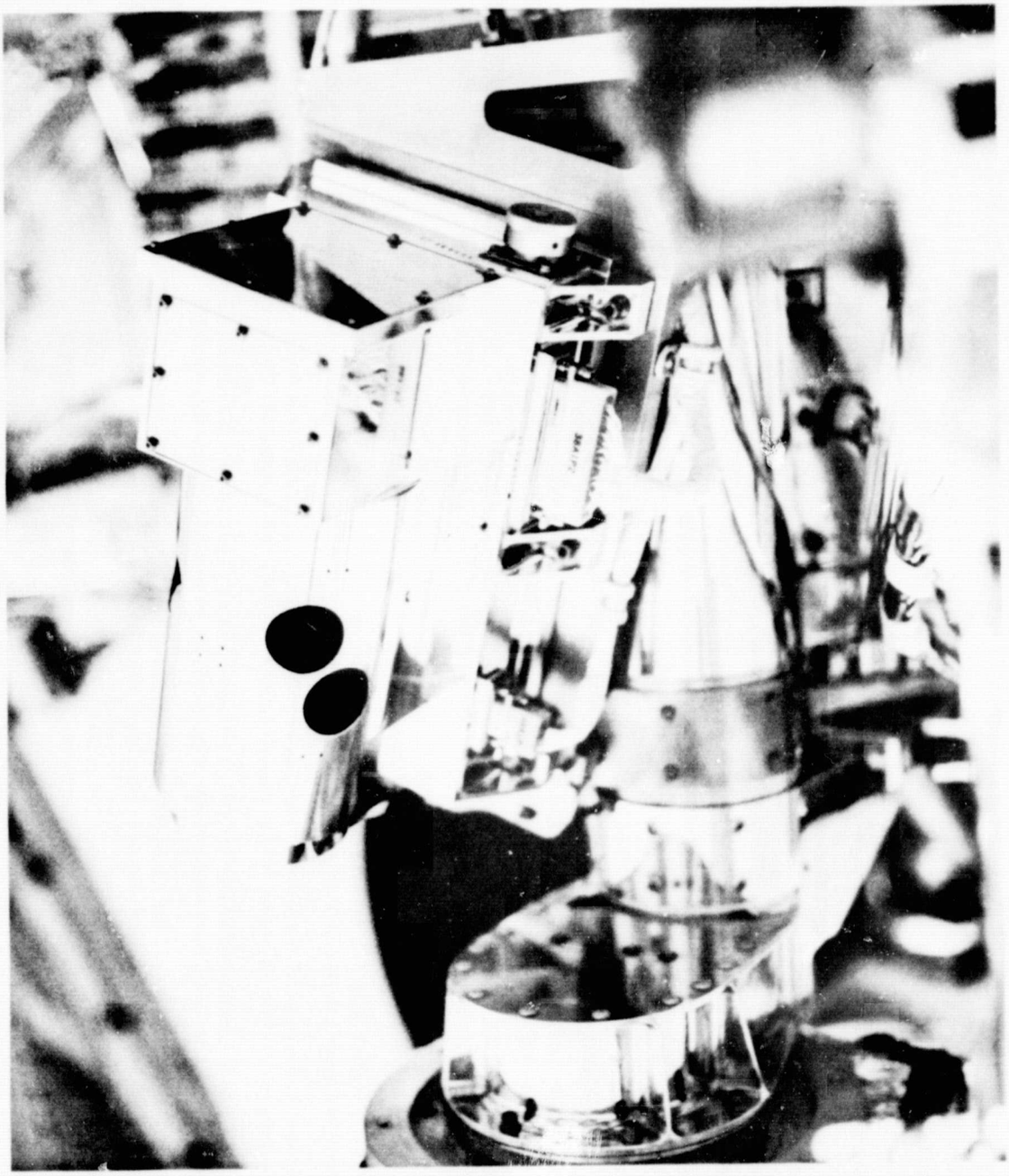

Figure 14. IRR Mounted, Before Thermal Blanket and Sunshield Installation

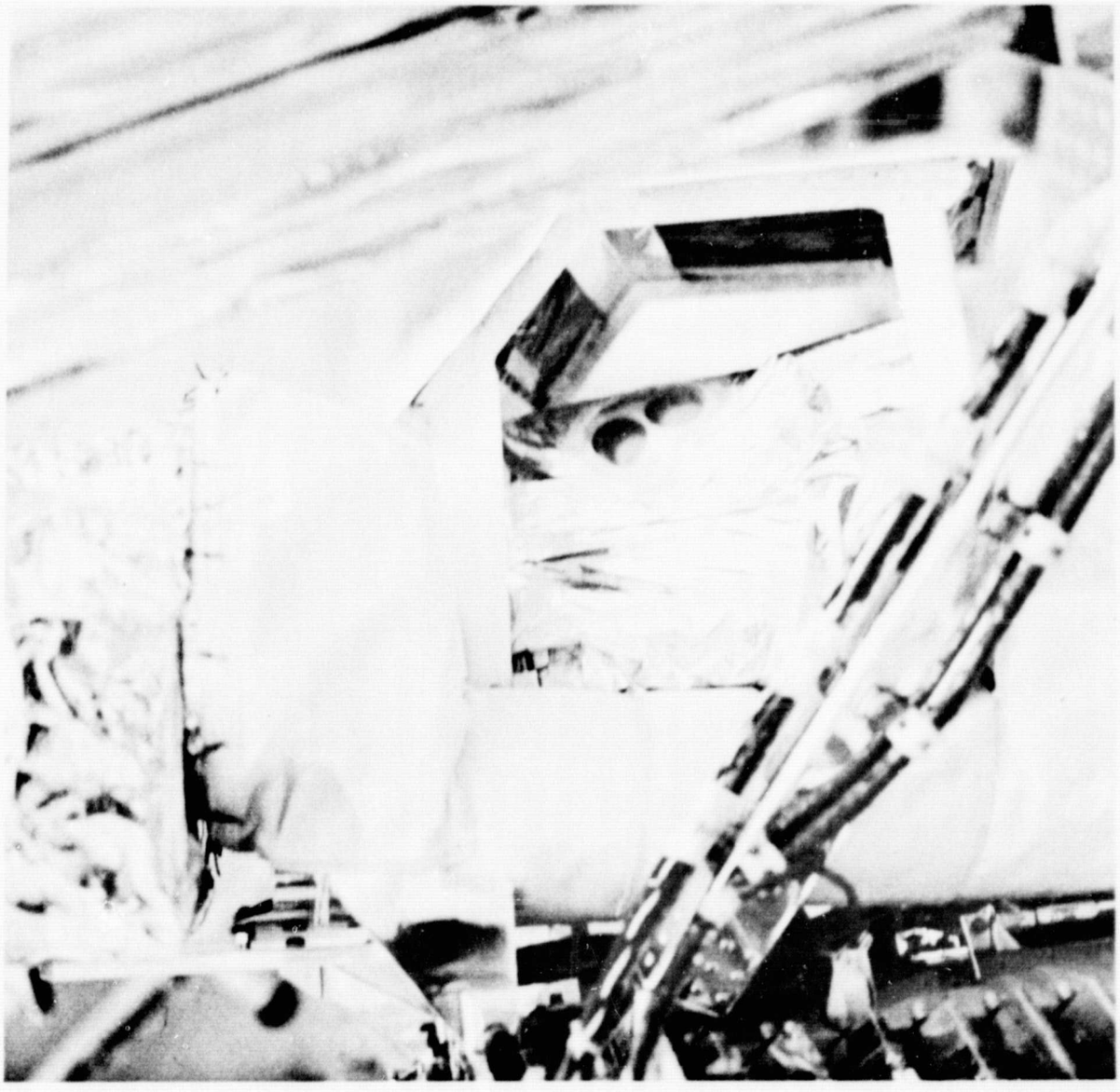

Figure 15. IRR After Thermal Blanket and Sunshield Installation

exposed radiating surface area of 103 cm^2 by cutting and hemming the IRR blanket which is wrapped around and under the IRR. This radiating area, determined by analysis and test, is predicted to maintain the IRR temperature within prescribed limits for the duration of the mission. As shown in Figure 13 the predicted IRR temperature agreed quite well with the actual IRR temperature for the mission.

3.4 Physical and Performance Parameters

The physical and performance parameters of the IRR MVM'73 are given in Table 3.

Table 3. IRR MVM'73 Performance Parameters

Parameter	Channel S	Channel L
Instantaneous FOV	0.5° round	1.07° round
Spectral Range	8.5 μm - 14 μm	34 μm - 55 μm
Brightness Temperature Range	200°K - 700°K	80°K - 320°K
Signal-to-Noise Ratio	27.2:1 at 200°K 3550:1 at 700°K	47:1 at 80°K 1850:1 at 320°K
NEΔT	0.32°K at 320°K 0.09°K at 700°K	0.21°K at 100°K 0.10°K at 320°K
Resolution	14 km at 1600 km	30 km at 1600
Detector		
Size	0.05 cm diam.	0.05 cm diam.
Time Constant	78 msec	78 msec
Resistance	9.6 kilohms	9.6 kilohms
Responsivity	267 volts/watt	267 volts/watt
System Bandwidth	0.64 Hz	0.64 Hz
Instrument		
Size	17.5 cm × 14.6 cm × 25.5 cm	
Weight	3.52 kilograms	
Power		
Avg. When Stepping	2.21 watts	
Stowed	2.7 watts	
Replacement Heater	2.5 watts	
Operating Temp. Range	-15.5°C to +35.5°C	
Storage Temp. Range	-30°C to +50°C	

4. TEST PROGRAM

The IRR was extensively tested on several levels. Electrical, electronic, optical, and mechanical components, circuits and subassemblies of the instrument itself were subjected to rigorous dimensional, fatigue, life, environmental, and other appropriate tests to ensure their flight quality for the IRR on the MVM'73 program.

Two flight quality radiometers were assembled from the flight qualified components, circuits, and subassemblies: a qualification or TA model, and a flight or FA model. The qual model was subjected to TA level subsystem environmental tests, which exposed the instrument to stresses much greater than the environmental stresses anticipated during the mission, and which in some instances were close to the design tolerance limits of the instrument. After these tests the qual model was refurbished to flight quality and retested to FA levels. The flight model was subjected to FA level subsystem environmental tests which exceeded the levels anticipated during the mission by small but tolerable levels. No refurbishment was required after the FA tests. The flight model was later flown to Venus and Mercury for a successful IRR science mission aboard the flight MVM'73 spacecraft.

After the subsystem tests both instruments were integrated onto MVM'73 spacecraft for system level testing, the qual model onto the 73-1 spacecraft and the flight model onto the 73-2 spacecraft.

The following two sections discuss in some detail the subsystem and system level tests, respectively, as they involved the IRR.

4.1 Subsystem Tests and Calibration

Subsystem testing of the IRR was carried out in accordance with the test programs specified in Reference 6, the detail environmental test spec for the IRR, and Reference 11, the SBRC environmental test plan for the IRR. An engineering breadboard model IRR was tested extensively at SBRC to help identify in advance problems which might arise with testing of the qual or flight models, and also to train SBRC test personnel in the test procedures to be used on those models. The qual model was subjected to TA level tests and the flight model to FA level tests.

The tests performed on the qual model, and the order in which they were performed are listed in Table 4. The tests performed on the flight model and the order in which they were performed are listed in Table 5.

Table 4. Qualification Model IRR Tests

1.	Bench Test
2.	Field-of-View Alignment and Stepping Accuracy
3.	Out-of-Band Sensitivity
4.	Initial Thermal-Vacuum Test
5.	Bench Test
6.	Vibration (sinusoidal and random)
7.	Bench Test
8.	Acoustical Noise
9.	Bench Test
10.	Field-of-View Alignment and Stepping Accuracy
11.	Thermal-Vacuum Test
12.	Thermal-Vacuum Calibration Check

Table 5. Flight Model IRR Tests

1.	Bench Test
2.	Field-of-View Alignment and Stepping Accuracy
3.	Out-of-Band Sensitivity
4.	Initial Thermal-Vacuum Test
5.	Bench Test
6.	Vibration Test (sinusoidal and random)
7.	Bench Test
8.	Field-of-View Alignment and Stepping Accuracy
9.	Thermal-Vacuum Test
10.	Thermal-Vacuum Calibration Check

The bench test is a performance verification check of the IRR at room ambient temperature and pressure. As seen from the test tables it was per-

formed once before and once after every environmental test to be sure there were no changes to the IRR as a result of the stresses imposed by the environmental test. The bench test checked the command functions, telemetry outputs, radiometric performance using a bench test thermal stimulus, and noise. The bench checkout equipment (BCE) used for the bench tests is shown in Figure 16. The bench test stimulus control unit in the BCE was used to control the bench and system test thermal stimulus, used for all nonthermal vacuum associated bench tests. The calibrator stimulus control unit was used to control the calibrated, vacuum qualified thermal stimuli, used for bench tests associated with the subsystem thermal vacuum tests and for calibration of the IRR. The radiometer control unit in the BCE performed the role of the FDS for the IRR during bench checkout. It provided the properly timed engineering, science, and channel select pulses to the IRR multiplexer for data sampling, and the command pulses for stepping and stowing the IRR scan mirror and for changing modes. A detailed description of the IRR BCE can be found in Reference 12.

The thermal stimulus used when bench testing (except for bench tests conducted during thermal vacuum tests) or systems testing the IRR is mounted directly onto the IRR as shown in Figure 17. The stimulus consists of two finned plates, approximating black bodies, one for each port. Only one plate can be heated. Since the other remains at room temperature the IRR restores on room temperature instead of on the near absolute zero of deep space for those tests in which this stimulus is used. In addition, except for the thermal vacuum tests, the detector assemblies are back filled with xenon gas, which provides a protective environment for the detectors and also provides a higher detector responsivity than would be possible in air or nitrogen. However, to develop full calibrated sensitivity the detectors must be in vacuum. Thus, before calibrations (which are done under thermal vacuum test conditions) or before launch the fill plugs, which normally seal off the xenon filled detector chambers, are removed. For the above reasons, and also because the stimulus temperature controller used with this stimulus is itself not accurately calibrated, the tests in which this stimulus is used do not yield calibrated data, but rather only a relative measure of instrument performance before and after exposure to an environmental test.

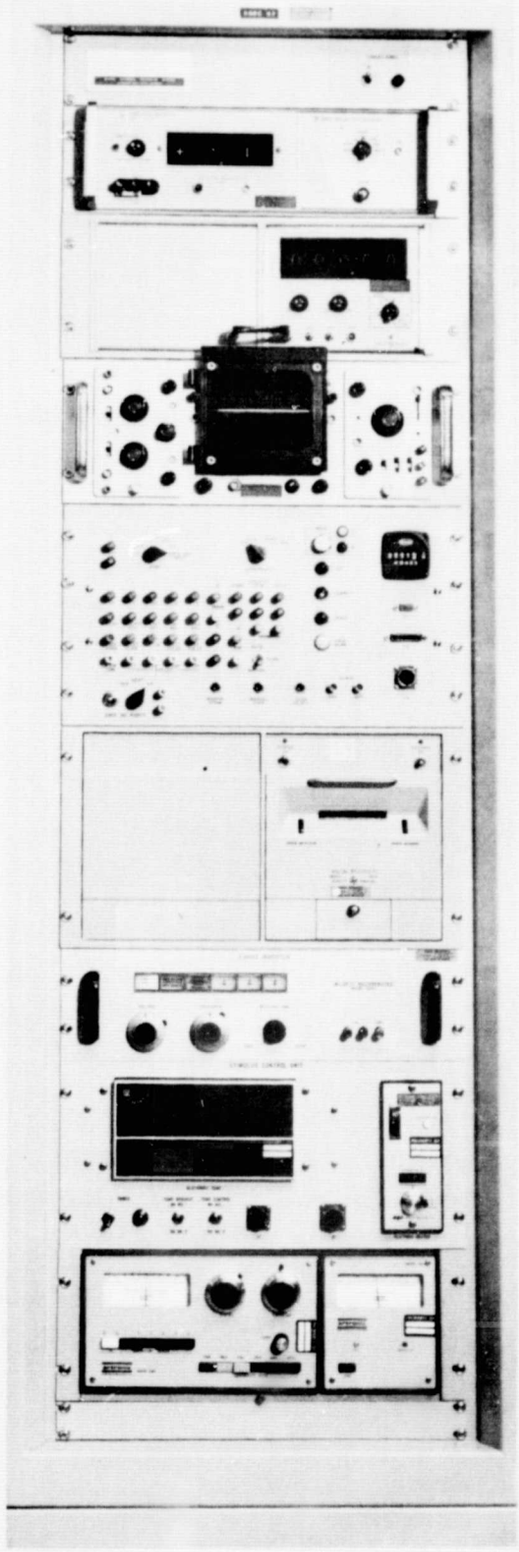

Figure 16. Bench Checkout Equipment for the Infrared Radiometer

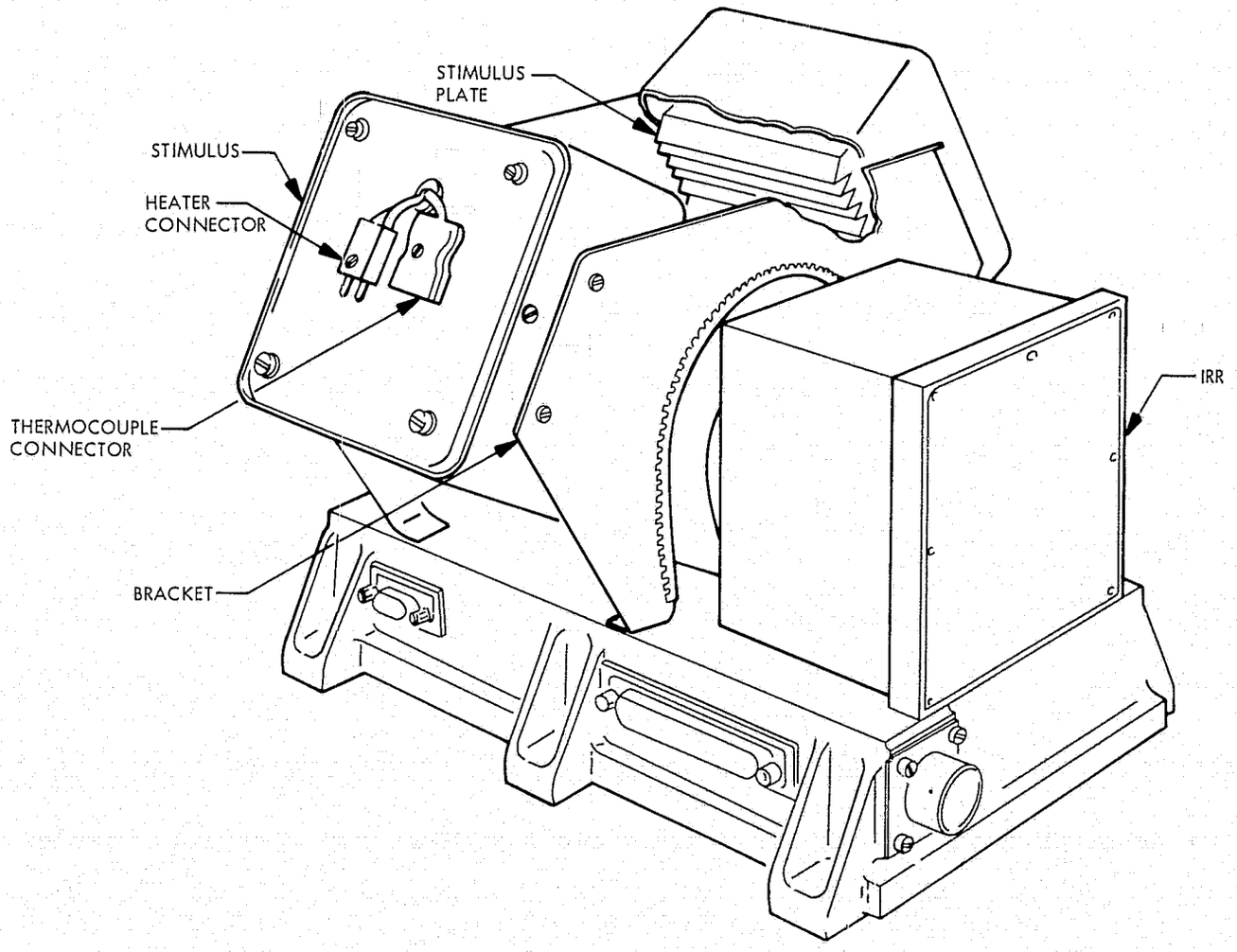

Figure 17. Bench Test Thermal Stimulus Mounted on IRR

FOV and stepping accuracy and repeatability measurements were made to ensure that the fore and aft IRR boresights relative to the IRR mounting surface (base plate) were within the allowed errors of ±0.067° clock and ±0.12° cone allocated to internal IRR sources (References 13 and 14). The measurements showed the boresights to be within tolerance both before and after the vibration and acoustics tests for the qual model and the vibration tests for the flight model.

The out-of-band sensitivity measurements were made to determine the spectral band shapes for the two channels, L and S, of the IRR. The results were discussed in the optics section, 3.1, of this report and are shown in Figures 5 and 6.

An initial thermal vacuum test was performed as an initial check of IRR radiometric performance in vacuum and to verify proper operation of the IRR command and telemetry functions. Resistor values necessary to set the channel gains and temperature compensating circuitry were also determined by the test. Channel gains were set such that the maximum brightness temperature measureable with channel L is approximately 320°K and with channel S approximately 700°K.

Both radiometers were subjected to sinusoidal and random vibration tests in each of three orthogonal directions in order to test their response to a simulated launch environment. The vibration test environments used are described below.

Qualification Model

Sinusoidal Test: Logarithmic sweep rate of 1 octave per minute from 5 to 2000 to 5 Hz at the following levels:

Frequency (Hz)	Acceleration (g - rms)
5 - 35	0.75
35 - 600	6.0
600 - 2000	3.0

Random Test: Vibrated 60 seconds in each axis. Instantaneous peak amplitudes ≥3 sigma were suppressed. The random vibration spectrum was as shown in Figure 18.

Flight Model

Sinusoidal Test: Logarithmic sweep rate of 3 octaves per minute from 5 to 2000 to 5 Hz at the following levels:

Frequency (Hz)	Acceleration (g - rms)
5 - 35	0.5
35 - 600	4.0
600 - 2000	2.0

Random Test: Vibrated 20 seconds in each axis. Instantaneous peak amplitudes ≥3 sigma were suppressed. The random vibration spectrum was as shown in Figure 18. The IRR undergoing the vibration test was rigidly attached to the vibration equipment by bolting the radiometer to a test fixture which was in turn bolted to the vibration equipment. The vibration test set up for the qual model is shown in Figure 19. A vibration survey of the test fixture with a simulated radiometer of the proper weight attached to it was conducted prior to the actual tests to ensure against unanticipated harmful resonances. Both instruments successfully passed the vibration tests, although sinusoidal vibration retest of the qual model was required in one axis because the channel L primary mirror (see Figure 4) came unbonded during the first test. This failure and others are discussed in Section 5, Problem Failure Reports.

The qual model only was subjected to an acoustic noise test. This test was designed to simulate the acoustic field present during launch. In the test the IRR was suspended in the center of the acoustic noise test chamber by soft suspension cords, with resonant frequency of the suspension mode less than 20 Hz, and subjected to the acoustic noise spectrum shown in Table 6. The test duration was 60 seconds. The IRR successfully passed this test.

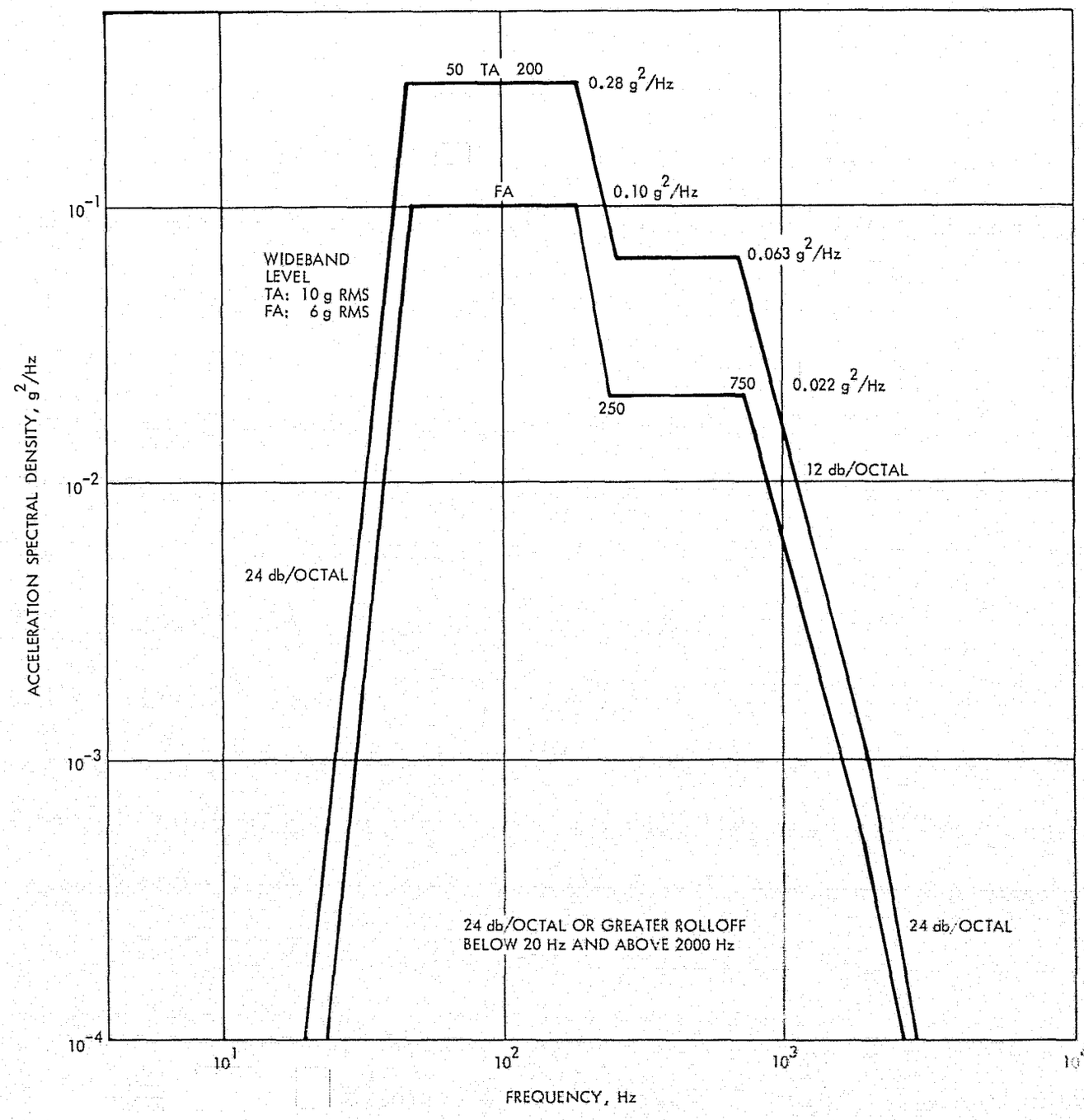

Figure 18. IRR Random Vibration Spectrum

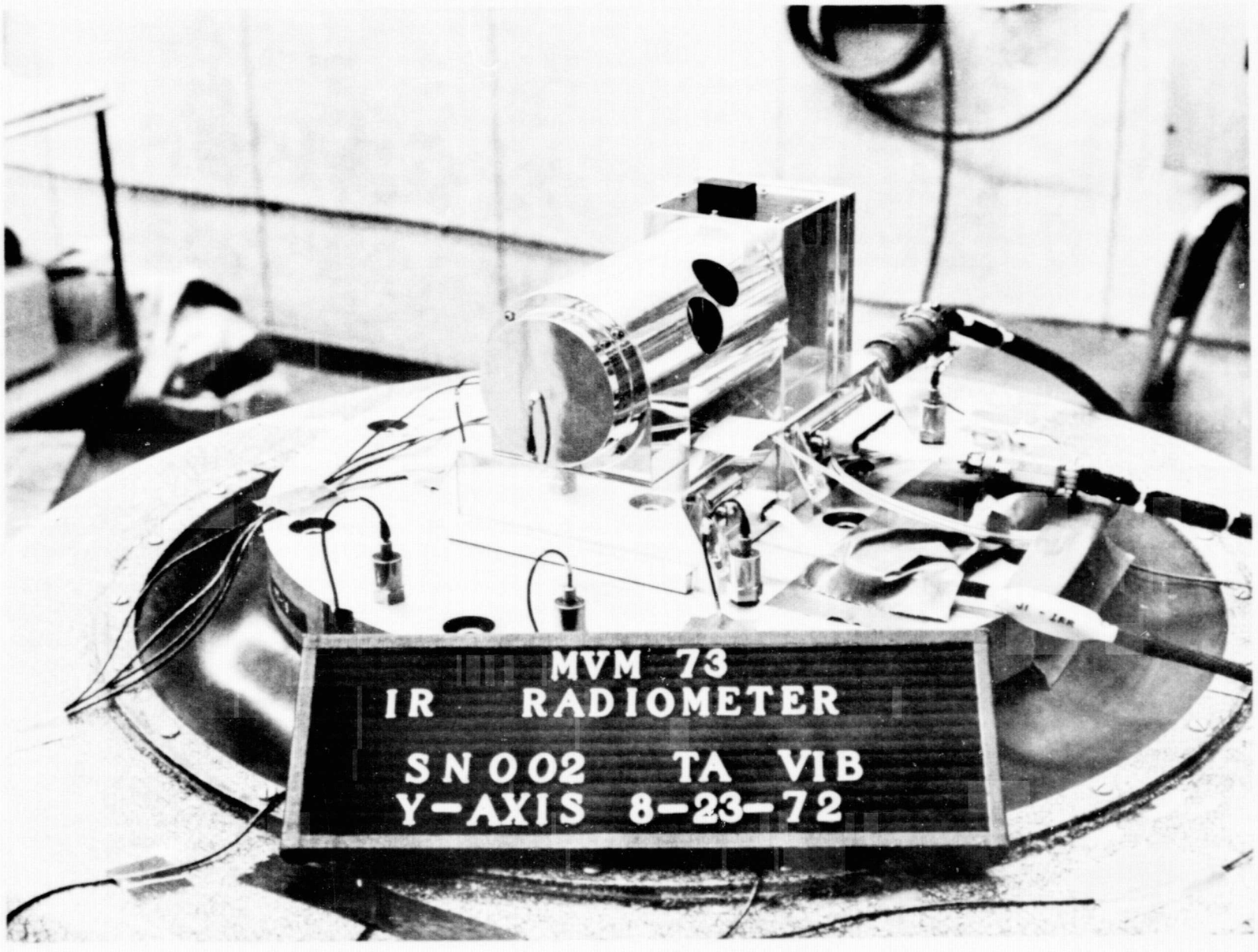

Figure 19. Vibration Test Set Up for the Qualification Model IRR

Table 6. Acoustic Test Spectrum for the Qualification Model IRR

1/3 Octave Band Center Frequency (Hz)	Sound Pressure Level (db) Referred to 2×10^{-9} N/cm^2	Tolerance (db) +	Tolerance (db) -
Overall	150.0	1	1
80*	131.5	3	3
100	134.0	3	3
125	137.0	3	3
160	139.5	3	3
200	142.0	3	3
250	142.0	3	3
315	142.0	3	3
400	142.0	3	3
500	139.0	3	3
630	135.5	5	3
800	132.0	7	3
1000	129.0	9	3
1250	125.5	11	3
1600	122.5	13	3
2000	119.5	15	3
2500	116.0	17	3
3150	112.5	19	3
4000	109.5	21	3
5000	106.0	23	3
6300	102.0	25	3
8000	99.0	27	3
10000**	95.5	29	3

*24 db/octave rolloff below 80 Hz.

**Above 10, 000 Hz, any 1/3 octave SPL shall not exceed 120 db.

Both radiometers were subjected to thermal vacuum tests in order to test their response to the high vacuum environment of space under instrument temperature conditions even more severe than those predicted for from near Earth to near Mercury. The thermal vacuum temperature profiles for the qual and flight model IRRs are shown in Figures 20 and 21 respectively. In all such tests the vacuum level was maintained at 1.33×10^{-3} N/m^2 (1×10^{-5} torr) or less.

The qual model suffered three separate detector failures during the tests. These failures are discussed in Section 5. Both IRRs ultimately passed the tests. After TA testing the qual model was refurbished and subjected to the FA level thermal vacuum tests, which it passed.

Calibration of the IRR involves the determination of radiometer responsivity over a range of instrument temperatures. Responsivity is defined as $\Delta DN/\Delta E$ where ΔDN is the difference in data number output corresponding to the difference in radiometer analog signal voltage developed between planet and space target looks, and ΔE is the difference in effective radiance between the planet and space targets. The target radiance as seen by the IRR is modified by the radiometer response curves, shown in Figures 5 and 6. Thus, the "effective radiance" of the target is a unique function both of the temperature of the target and the spectral response of the IRR. Tables of effective radiance versus target temperature were generated by SBRC for both channels of the IRR.

The responsivity of both IRR channels was determined over the instrument temperature range -20°C to +40°C in 10°C steps. Two calibrated vacuum qualified thermal stimuli with thermal stability better than 0.01°K served as the planet and space targets for the calibration. In order to establish the constancy of the responsivity for a given instrument temperature several measurements were made at each instrument temperature. The space target was kept fixed at around 80°K for all measurements and the planet target was varied between 115°K and 700°K in prescribed increments (Reference 15). For each pair of target temperatures (one space and one planet) a corresponding pair of effective radiances was determined from the above mentioned tables, and, using the associated pair of DN readings, a value for responsivity determined. Plots showing the calibration data for both channels, and the least

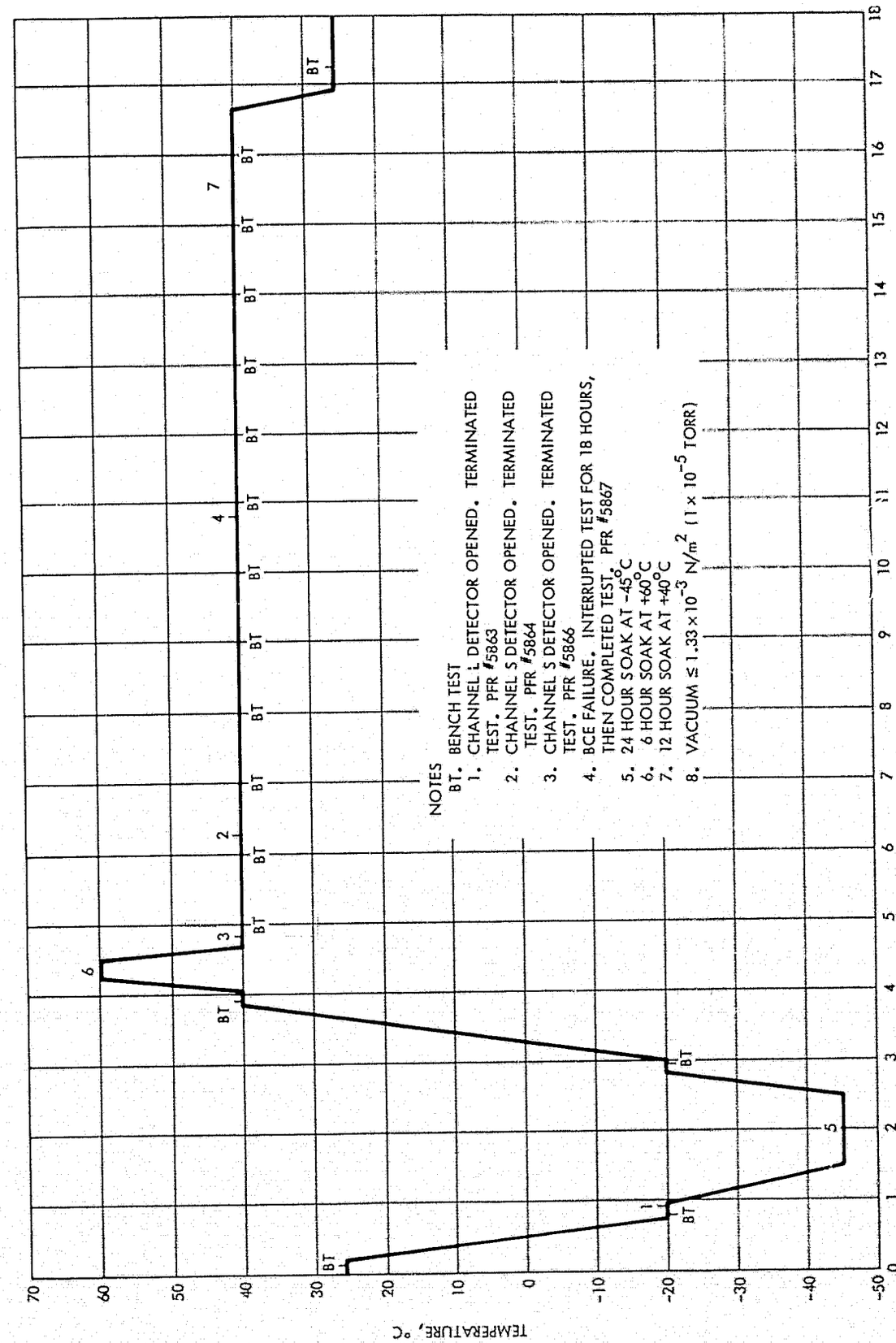

Figure 20. TA Level Thermal Vacuum Test and Temperature Profile for the IRR

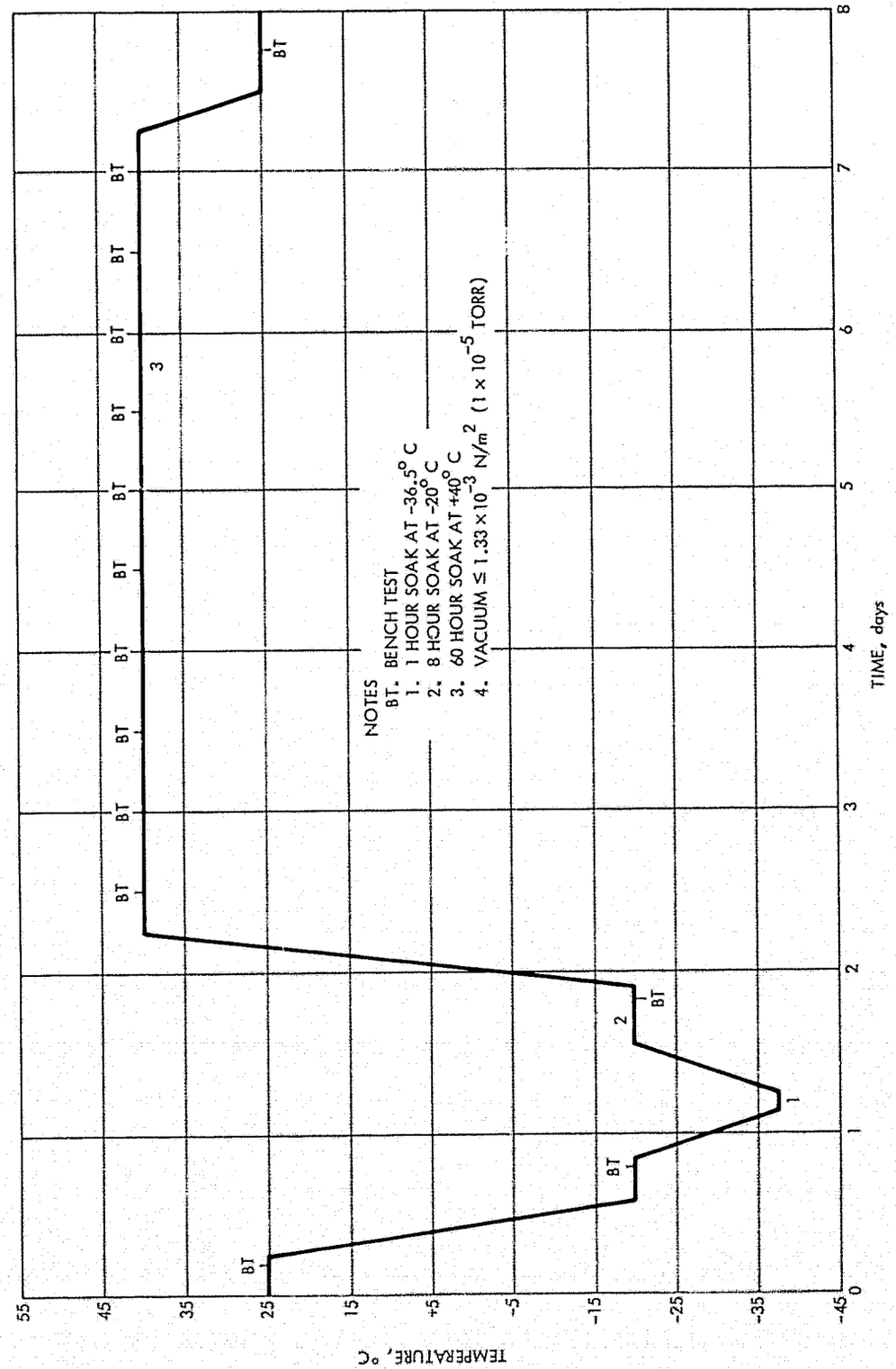

Figure 21. FA Level Thermal Vacuum Test and Temperature Profile for the IRR

squares curves associated with that data, for the flight model IRR are given in Figures 22 and 23 (Reference 16).

As an example of the use of the calibration consider the case shown in Figure 10 and discussed in Section 3.2.3. Assume the +2 volt analog signal there, which yielded +200 DN, was the result of a planet measurement in channel L and that the associated space measurement yielded -498 DN, which is normal. Suppose furthermore that the instrument temperature was +25°C. From Figure 23 the inverse responsivity corresponding to an instrument temperature of +25°C is

$$\frac{\Delta E}{\Delta DN} = 8.325 \times 10^{-7} \text{ watt/cm}^2 \text{ - steradian.}$$

From the above data we have

$$\Delta DN = 200 - (-498) = 698.$$

Thus,

$$\Delta E = 5.81 \times 10^{-4} \text{ watt/cm}^2 \text{ - steradian.}$$

The value of radiance for space is negligible compared to that for a target that yields a data point of 200 DN. Thus, from the effective radiance table for channel L, the brightness temperature corresponding to 200 DN is

$$T = 252.7°K.$$

4.2 System Tests and Alignment Verification

The primary objective of system level testing of the spacecraft as it pertained to the IRR was to verify, within the bounds of test practicality, that the IRR, integrated onto the spacecraft, would perform the functions necessary for it to achieve a successful mission. System testing as it related to the IRR was divided into several phases as listed in Table 7.

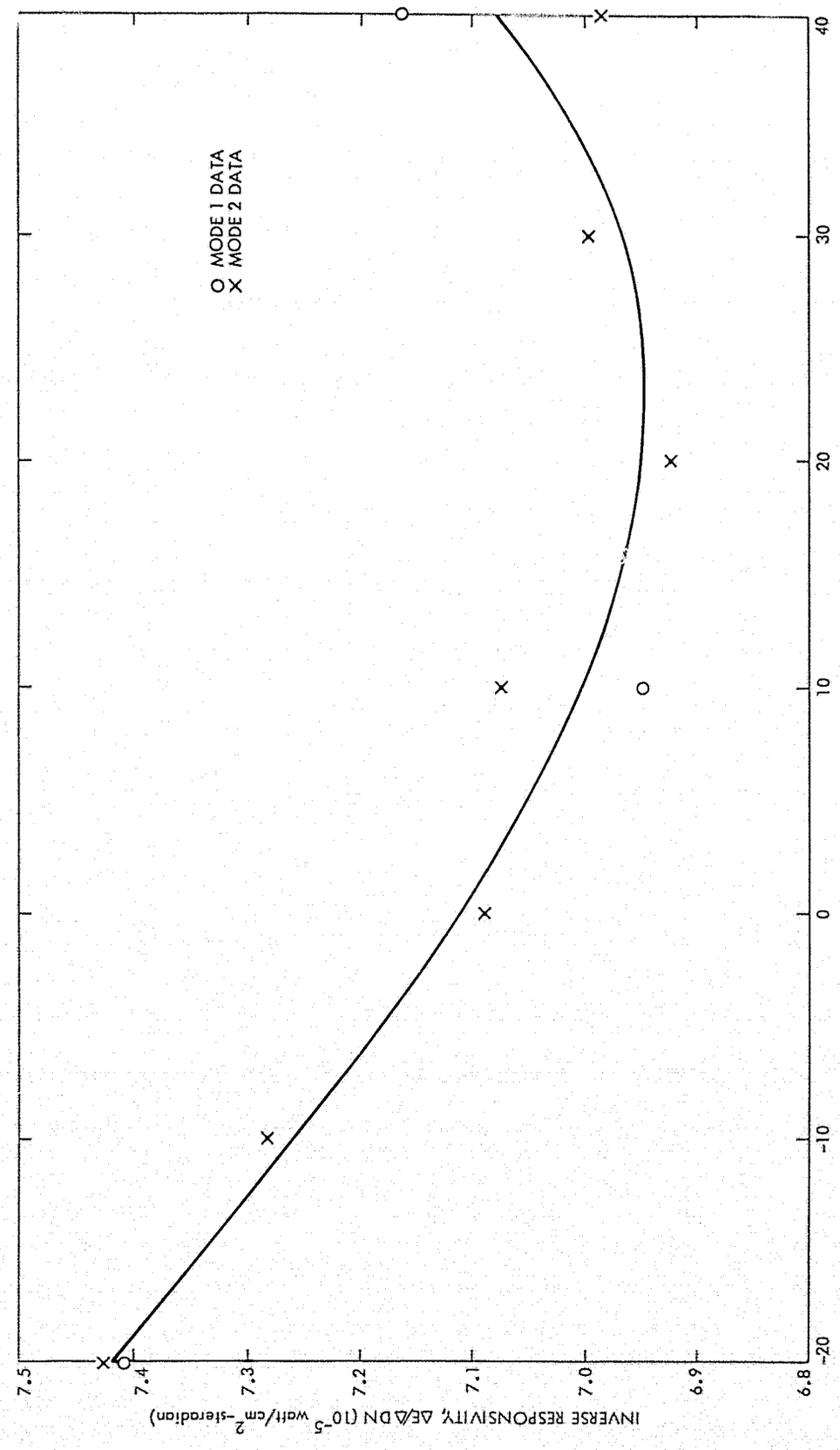

Figure 22. IRR Channel S Calibration Curve

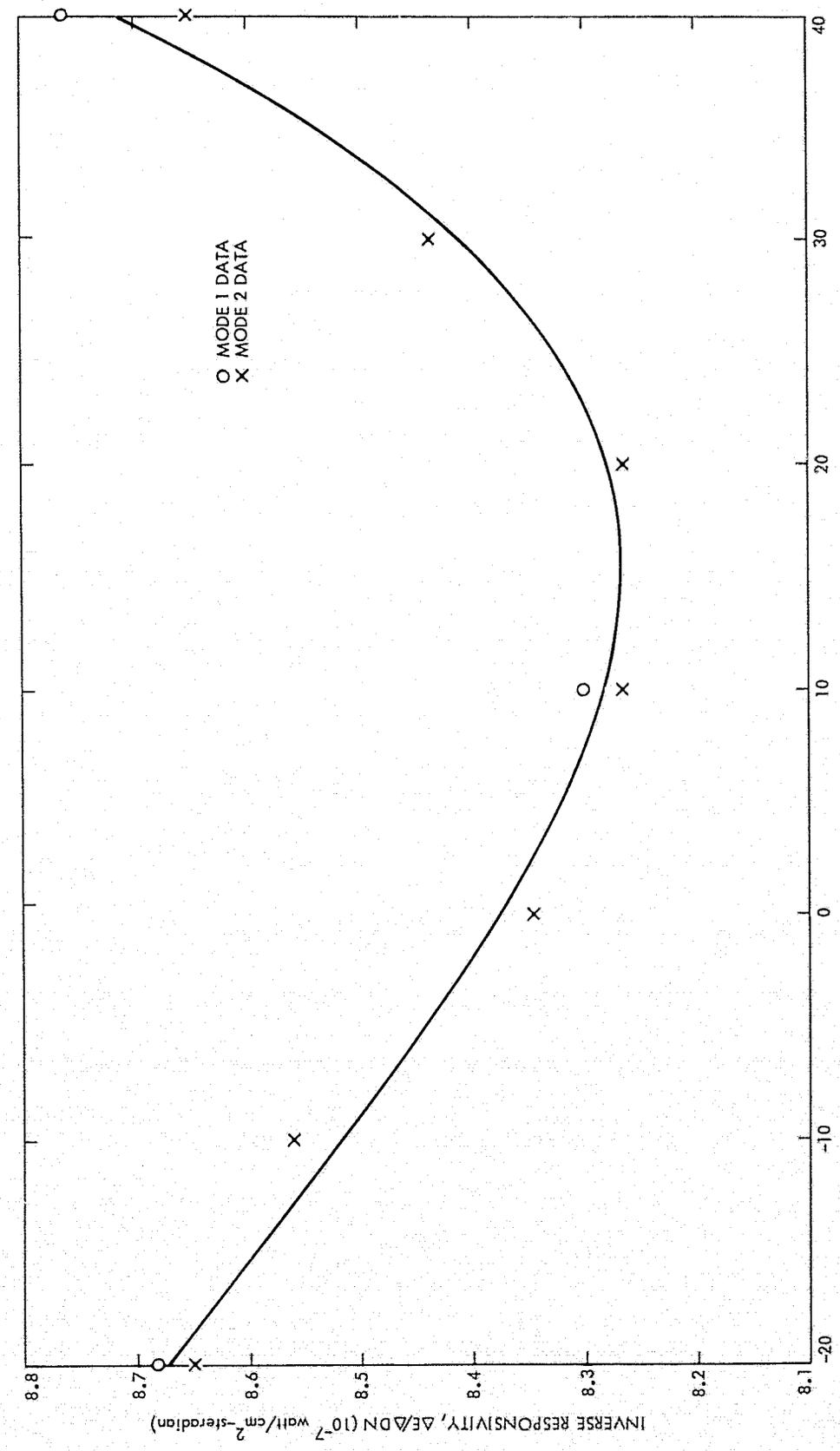

Figure 23. IRR Channel L Calibration Curve

Table 7. System Level Test Phases Involving the IRR

1. Integration
2. System Tests
   - IRR Performance
   - Encounter Sequence
   - S/C Readiness Test
   - S/C Intra-Action Test
3. Alignment
4. S/C Operational/Functional Tests (SOFT)
5. Vibration
6. Solar Thermal Vacuum

System level testing was accomplished at three locations: the Spacecraft Assembly Facility (SAF) at The Boeing Company in Seattle, the Jet Propulsion Laboratory, and the Air Force Eastern Test Range (AFETR) at Cape Canaveral. Integration, system tests, alignment, vibration, and SOFT tests were conducted at The Boeing Company. Solar thermal vacuum testing and associated SOFT type tests were conducted at JPL. At AFETR, in addition to SAF type system testing at an ambient environment, tests were conducted in the explosive safe facility and on the launch pad in launch configuration.

The IRR interfaced with other science subsystems and the spacecraft for the first time in the SAF at The Boeing Company. Except for the never fully explained appearance of anomalously high current pulses seen by the power subsystem during integration of the qual model IRR onto the backup (73-1) spacecraft there were no major problems relating to the IRR during system level testing. All system level PFRs relating to the IRR, as well as those PFRs generated on the subsystem level, are discussed in Section 5.

The alignment verification tests were performed with the flight model IRR mounted on the flight spacecraft. The test was performed before and after system level vibration testing. The test consisted of theodolite measurements of the IRR forward and aft boresights relative to the spacecraft axes using an autocollimating mirror mounted to the backside of the IRR channel S secondary mirror as shown in Figure 4. The measured boresight pointing

angles were translated into cone and clock angles and then compared with the required nominal boresight angles to determine if the alignment was within tolerance both before and after the vibration tests.

The required nominal boresight pointing angles with their allowed tolerances for the forward boresight are

$$C_F = 60.20°, \qquad \Delta C_F = \pm 0.35°$$

$$K_F = 246.91°, \qquad \Delta K_F = \pm 0.15°$$

and for the aft boresight are

$$C_A = 60.20°, \qquad \Delta C_A = \pm 0.35°$$

$$K_A = 71.15°, \qquad \Delta K_A = \pm 0.15°$$

where C is cone and K is clock angle and ΔC and ΔK are the allowed tolerances. Before system level vibration the alignment verification measurements on the IRR yielded (Reference 17) for the forward boresight

$$C_{Fbv} = 60.23°, \qquad \Delta C_{Fbv} = + 0.03°$$

$$K_{Fbv} = 246.775°, \qquad \Delta K_{Fbv} = - 0.135°,$$

and for the aft boresight

$$C_{Abv} = 60.254°, \qquad \Delta C_{Abv} = + 0.054°$$

$$K_{Abv} = 74.078°, \qquad \Delta K_{Abv} = - 0.072°,$$

all within the allowed tolerances. The figures given here for the aft boresight measurements are an average of three measurements, (1) as installed alignment, (2) after PSE/IRR boom deployment to check boom deployment repeatability, and (3) after removing and replacing the IRR on its mount to check

installation alignment repeatability. All three measurements were also within the allowed tolerances.

After system level vibration the alignment verification measurements on the IRR yielded (Reference 18) for the forward boresight

$$C_{Fav} = 60.191°, \qquad \Delta C_{Fav} = -0.009°$$

$$K_{Fav} = 246.857°, \qquad \Delta K_{Fav} = -0.053°,$$

and for the aft boresight

$$C_{Aav} = 60.214°, \qquad \Delta C_{Aav} = +0.014°$$

$$K_{Aav} = 74.239°, \qquad \Delta K_{Aav} = +0.089°,$$

all well within the allowed tolerances.

The solar thermal vacuum (STV) tests required, for the IRR, a pair of special thermally protected stimuli, an elaborate stimuli deployment structure, and an STV IRR stimuli thermal control console. The stimuli themselves are 12.7 cm diameter thermal blanket protected cylindrical black bodies. Except for the thermal protection, which is unique to the MVM'73 IRR STV thermal requirements, the stimuli are residual IRR and IRIS stimuli from the MM'71 program.

The deployment structure is mechanized with the stimuli mounted at the end of a long deployable rod. When stowed the whole structure is close to the cooled STV chamber walls, out from under the solar beam as shown in Figure 24. When deployed both stimuli move into the solar beam and into the FOV of the IRR, but in such a way that only one stimulus (the stimuli are identified as the forward port stimulus, and the aft port stimulus) can be seen by the IRR at a time. Depending on whether the IRR is being tested in mode 1 or mode 2, the forward or aft port stimulus respectively is deployed into the appropriate IRR FOV.

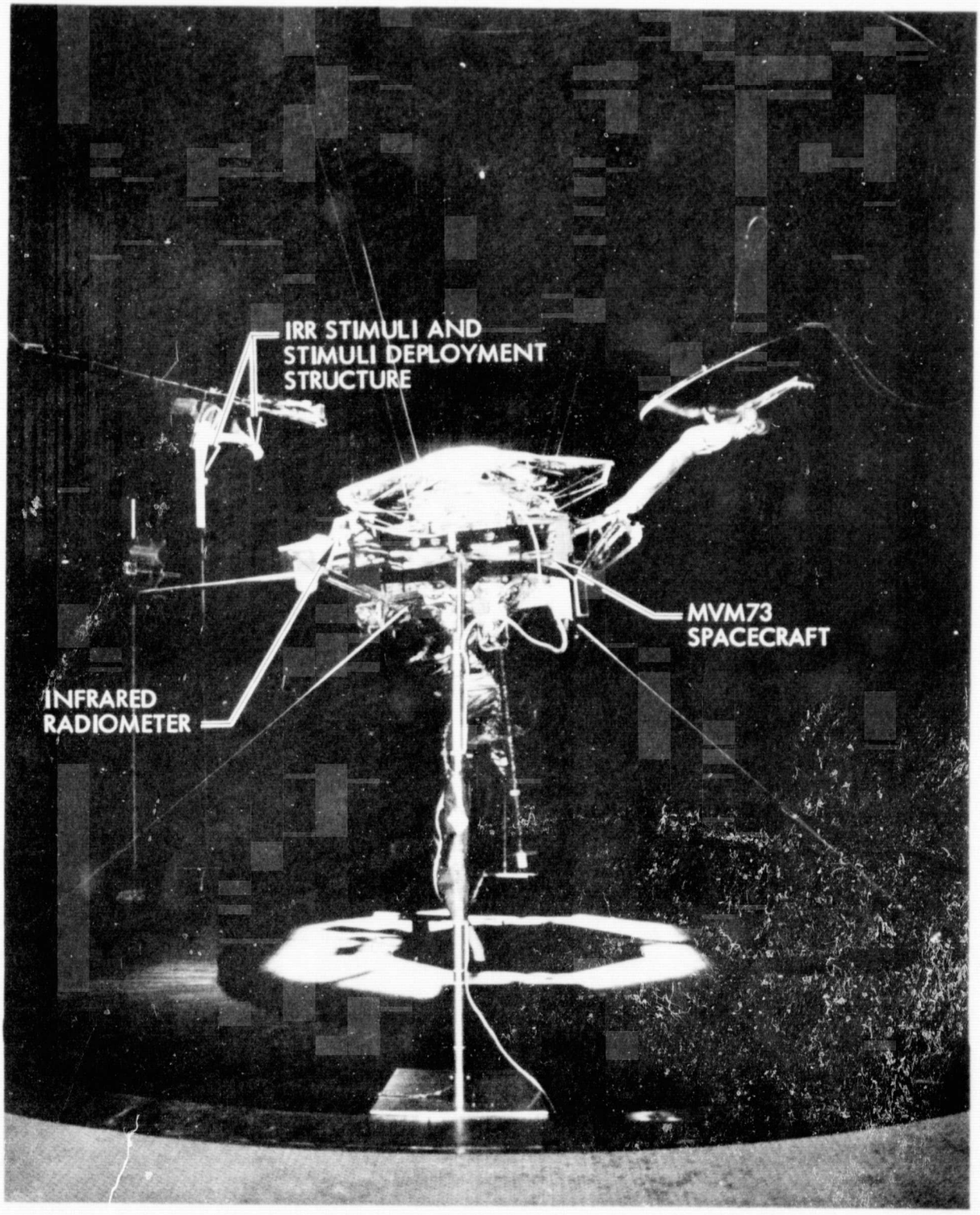

Figure 24. MVM '73 STV Test Set Up Showing IRR Stimuli Structure Stowed

The STV IRR stimuli thermal control console is shown in Figure 25. Stimulus temperature is read out directly on the associated DVM with resolution of 0.1°C. The stimuli were calibrated from -15°C to +120°C (Reference 19). During the STV tests the IRR performance was tested at STV solar constants of 2.0 suns and 4.8 suns with stimulus temperatures set at 0°C, 40°C, 80°C and 120°C. All the IRR STV tests were successful.

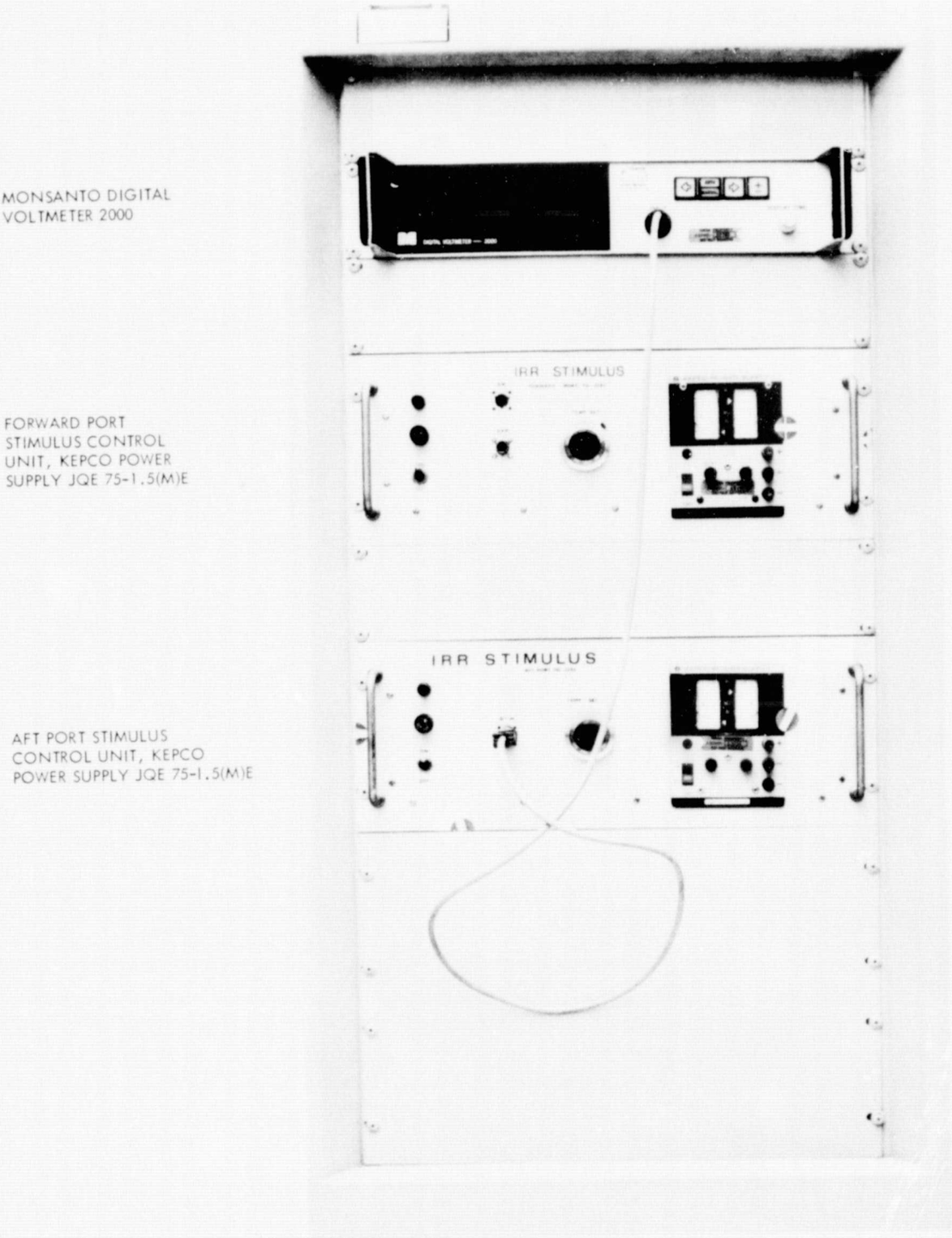

Figure 25. IRR Stimuli Temperature Control Console for the Solar Thermal Vacuum Tests

5. PROBLEM FAILURE REPORTS

There are a total of 11 problem failure reports (PFRs) written against the qual model IRR. Seven of these PFRs were written at the subsystem level, before delivery of the IRR to SAF at The Boeing Company for system level testing. The other four were written after delivery to SAF. The nature and resolution of the PRFs written against the qual model IRR are given in Table 8.

There are a total of five PFRs written against the flight model IRR. Two of these PFRs were written before delivery of the flight model IRR to SAF for system level testing. The other 3 were written afterwards. The nature and resolution of the flight model IRR PFRs are given in Table 9.

Table 8. Qualification Model IRR Problem Failure Report Summary

PFR No.	Date Initiated	PFR Description	Resolution	Date Closed
5861 Subsystem Level	8/23/72	Primary mirror from channel 1 came disbonded during TA level vibration tests.	Mirror was rebonded and static tested to 100 g's. Reassembled IRR was then vibrated to TA level in Z-axis only.	10/13/72
5862 Subsystem Level	8/23/72	Scratch on polished surface of IRR.	Cosmetic effect only. Since IRR is covered by thermal blanket during mission, no impact. No action required. None taken.	11/14/72
5863 Subsystem Level	9/19/72	Channel 2 detector opened during TA level thermal/vac tests.	Debris in detector chamber. Chamber cleaned out and screen put over xenon fill holes.	10/11/72
5864 Subsystem Level	9/25/72	Channel 1 detector opened during TA level thermal/vac tests.	Detector fabrication process modified to give 50% thicker thermopile, grounding techniques improved, and protective diodes incorporated to eliminate overvoltage possibility.	2/11/73
5865 Subsystem Level	9/25/72	Channel 1 detector found to be defective during bench checkout of IRR.	Static discharge caused defective detector. Same resolution as for PFR 5864	12/6/72
5866 Subsystem Level	10/1/72	Channel 1 detector opened during TA level thermal/vac tests.	Same resolution as for PFR 5864.	2/11/73

Table 8. (cont'd)

PFR No.	Date Initiated	PFR Description	Resolution	Date Closed
5867 Subsystem Level	10/20/72	Erratic behavior of channel 2 dc restore circuit during TA level thermal/vac tests.	Noise in BCE caused science select pulse to occur early thus affecting dc restore circuit. Replaced noisy BCE circuit.	2/9/73
3065 System Level	11/27/72	Power subsystem recorded anomalously high current pulses coinciding with IRR step pulses during IRR integration onto the 73-1 spacecraft.	No ill effects to IRR or any other subsystem noted because of current pulses. Unable to reproduce phenomenon. Problem ascribed to sinister force.	7/30/73
3066 System Level	1/12/73	Anomalous data observed in IRR output during systems level power profile test.	MTC problem. No action against IRR required. None taken.	4/5/73
3067 System Level	1/22/73	Loose nut inside system test thermal stimulus.	Standoff insulators broken inside stimulus. Necessary repairs made.	3/13/73
3187 System Level	5/14/73	IRR response to thermal stimulus out of tolerance.	Caused by loss of xenon from detector chamber. Calibration unaffected. Recharged with xenon. No other action required or taken.	8/10/73

Table 9. Flight Model IRR Problem Failure Report Summary

PFR No.	Date Initiated	PFR Description	Resolution	Date Closed
5868 Subsystem Level	1/2/73	During FA level vibration testing at JPL, shaker table hit the stops at the end of each sine sweep.	IRR was bench checked extensively to ensure no deleterious impulses were coupled into the instrument. IRR checked out OK. No action required by IRR. None taken. PFR 5869 was written against the shaker facility. It was repaired as needed.	3/7/73
5870 Subsystem Level	1/9/73	During FA level thermal/ vac testing, while cooling one of the calibrated thermal stimuli, LN_2 line inside vac chamber ruptured causing sudden loss of pressure.	Chamber repairs were made. No noticeable effects to IRR. Test resumed and successfully concluded. No action required by IRR. None taken.	2/11/73
3121 System Level	3/12/73	Stimulated response of the IRR to system test thermal stimulus was different than that obtained during bench tests. Also very erratic.	Temperature controller in BCE replaced. Stability restored.	5/4/73
3162 System Level	4/13/73	Stimulated response of the IRR to system test stimulus out of tolerance.	Caused by loss of xenon from detector chamber. Calibration unaffected. Recharged chamber with xenon. No other action required. None taken.	7/30/73
3328 System Level	8/1/73	Light amber contaminant coating over IRR surface observed during post STV test visual inspection.	IRR cleaned with acetone swab. No optics contamination detected. After STV test nonflight tape and wire removed from IRR. No other action required. None taken.	10/8/73

REFERENCES

1. The "science objectives" information in the introduction was taken primarily from the original proposal entitled "Infrared Radiometer Experiment for the 1973 Mariner Venus/Mercury Mission" submitted to NASA, MVM Program Office, Washington, D. C. by Santa Barbara Research Center, May 21, 1970 (internal document).

2. "Functional Requirement, Mariner, Venus/Mercury 1973, Infrared Radiometer," Boeing Document No. MVM73-4-2038, T. C. Clarke, November 10, 1971 (internal document).

3. "Design Requirement, Mariner Venus Mercury 1973 Flight Equipment, Flight Data Subsystem," JPL Document No. MVM73-2006-1, Revision B, P. B. Whitehead, pages 186-189, September 9, 1971 (JPL internal document).

4. "A/PW Converter Users Guide," Attachment to JPL Interoffice Memorandum Design File: MM'71-10-4, "Some Precautions to Observe When Using an A/PW Converter," Jack Collier, September 26, 1969 (JPL internal document).

5. Logbook, IRR Flight Instrument, MVM'73, Santa Barbara Research Center (internal document).

6. "Infrared Radiometer Subsystem, Type Approval and Flight Acceptance Testing, Mariner Venus/Mercury 1973 Flight Equipment Detail Specification for," Spec. No. TS 506642, Rev. A, T. C. Clarke, July 20, 1972, Jet Propulsion Laboratory, Pasadena, California (JPL internal document).

7. "Pre SAF Hardware Review, MVM'73 Infrared Radiometer Serial No. 001, Flight Model," T. C. Clarke, Instrument Coordinator, The Boeing Company, March 15, 1973 (internal document).

8. "PSE/IRR Thermal Interaction," Boeing Coordination Sheet EM-TC-226, R. K. MacGregor to G. N. Davison, December 18, 1972 (internal document).

9. "Expected Flight Temperature Predictions," Boeing Coordination Sheet EM-TC 296, R. K. MacGregor to Distribution 103A, August 29, 1973 (internal document).

10. "IRR Temperature Flight Data for November 3, 1973 Through March 29, 1974," attached to Interoffice Memorandum 3533 MVM-74-046, "Mariner 10 Temperature Control Performance, L+110 Days Through L+165 Days," R. A. Becker to W. I. Purdy, June 18, 1974 (JPL internal document).

11. "Environmental Test Plan, Mariner Venus Mercury 1973, Infrared Radiometer," Revision B, SBRC Document No. ERE 72/49, A. R. Davis, July 18, 1972, Santa Barbara Research Center, Goleta, California (internal document).

12. "Support Equipment, Functional Requirements, Mariner Venus/Mercury 1973, Infrared Radiometer," Boeing Document No. MVM73-4-2138, T. C. Clarke, February 29, 1972 (internal document).

13. "IRR Alignment Accuracy Requirements and Allocations," Boeing Memo 2-1083-SSE-535, D. Stoddard to J. W. Bolender, et. al., March 31, 1972 (internal document).

14. "Functional Requirement, Mariner Venus/Mercury 1973 Spacecraft, Functional Accuracies," Boeing Document No. MVM73-3-160B, D. B. Stoddard, July 7, 1972 (internal document).

15. "Radiometric Calibration Specification/Procedure - Mariner Venus/Mercury 1973 - Infrared Radiometer," Santa Barbara Research Center Document No. 19457, J. L. Engel, October 27, 1972 (internal document).

16. From correspondence providing the absolute temperature conversion coefficients for the flight model IRR, Jet Propulsion Laboratory, Division 825 correspondence, E. D. Miner to T. C. Clarke, February 15, 1973 (JPL internal document).

17. "Results of IRR Alignment Verification," MVM JPL Field Office Memo No. 130, T. C. Clarke to C. M. Yeates, March 27, 1973 (JPL internal document).

18. "Post Vibration Alignment Verification of the IRR," MVM JPL Field Office Memo No. 241, T. C. Clarke to C. M. Yeates, June 25, 1973 (JPL internal document).

19. "IRR STV Stimuli Calibration," MVM JPL Field Office Memo No. 242, T. C. Clarke to D. Swenson, June 28, 1973 (JPL internal document).